International Journal of Nanomedicine

Dovepress
open access to scientific and medical research

Open Access Full Text Article

REVIEW

Recent Advances in Intranasal Administration for Brain-Targeting Delivery: A Comprehensive Review of Lipid-Based Nanoparticles and Stimuli-Responsive Gel Formulations

Jain Koo[1,2], Chaemin Lim[3], Kyung Taek Oh[1,2]

[1]Department of Global Innovative Drugs, The Graduate School of Chung-Ang University, Seoul, Republic of Korea; [2]College of Pharmacy, Chung-Ang University, Seoul, Republic of Korea; [3]College of Pharmacy, CHA University, Seongnam-si, Gyeonggi-do, Republic of Korea

Correspondence: Kyung Taek Oh; Chaemin Lim, Tel/Fax +82-2-824-5617, Email kyungoh@cau.ac.kr; chaemin@cha.ac.kr

Abstract: Addressing disorders related to the central nervous system (CNS) remains a complex challenge because of the presence of the blood-brain barrier (BBB), which restricts the entry of external substances into the brain tissue. Consequently, finding ways to overcome the limited therapeutic effect imposed by the BBB has become a central goal in advancing delivery systems targeted to the brain. In this context, the intranasal route has emerged as a promising solution for delivering treatments directly from the nose to the brain through the olfactory and trigeminal nerve pathways and thus, bypassing the BBB. The use of lipid-based nanoparticles, including nano/microemulsions, liposomes, solid lipid nanoparticles, and nanostructured lipid carriers, has shown promise in enhancing the efficiency of nose-to-brain delivery. These nanoparticles facilitate drug absorption from the nasal membrane. Additionally, the in situ gel (ISG) system has gained attention owing to its ability to extend the retention time of administered formulations within the nasal cavity. When combined with lipid-based nanoparticles, the ISG system creates a synergistic effect, further enhancing the overall effectiveness of brain-targeted delivery strategies. This comprehensive review provides a thorough investigation of intranasal administration. It delves into the strengths and limitations of this specific delivery route by considering the anatomical complexities and influential factors that play a role during dosing. Furthermore, this study introduces strategic approaches for incorporating nanoparticles and ISG delivery within the framework of intranasal applications. Finally, the review provides recent information on approved products and the clinical trial status of products related to intranasal administration, along with the inclusion of quality-by-design–related insights.

Keywords: nose to brain delivery system, lipid based nanoparticle, in situ gel, bypassing BBB

Introduction

Global healthcare data indicate a significant increase in the prevalence of central nervous system (CNS) diseases, which contribute approximately 6–8% to the global economy.[1] Over time, the incidence of conditions such as Alzheimer's disease, Parkinson's disease, schizophrenia, multiple sclerosis, and CNS cancers has markedly increased.[2–6] Despite this trend, conventional treatments for CNS disorders have predominantly relied on administration routes that target peripheral areas, such as oral and parenteral methods.[7] However, the efficacy of therapeutic agents faces considerable hurdles due to the complex blood-brain barrier (BBB). Although intracerebroventricular injection has emerged as an alternative approach, its invasive nature, associated discomfort, and limited practicality have restricted its use to specialized medical contexts.

The BBB is a highly specialized and tightly regulated semipermeable barrier that separates circulating blood from the brain's extracellular fluid.[8–11] It is primarily composed of endothelial cells lining the blood vessels in the brain and is surrounded by additional support cells such as astrocytes. The BBB plays a crucial role in maintaining the

Received: 19 October 2023
Accepted: 23 January 2024
Published: 23 February 2024

microenvironment of the brain by controlling the passage of substances between the blood and brain tissue. This barrier selectively allows essential nutrients and molecules to pass through, while restricting the entry of potentially harmful substances, pathogens, and most large molecules. Its unique structure and function make it a significant challenge to deliver drugs and therapeutic agents to the brain, requiring innovative strategies for the effective treatment of CNS disorders.

Therefore, intranasal administration has attracted considerable research interest as an alternative method to conventional parenteral and oral routes, because it can increase the drug concentrations in the brain by direct nose-to-brain delivery via olfactory and trigeminal nerve pathways. This additionally ensures a rapid onset of action, it circumvents hepatic first-pass effects, and provides a patient-friendly administration route.[7,12,13] To increase the efficacy of nose-to-brain delivery, nanoparticles have emerged as promising carriers because of their remarkable capacity to facilitate drug transportation.[14] Nanoparticles improve drug stability by encapsulating them within a matrix and protecting them from extracellular transport via P-glycoprotein efflux proteins. They can also be transported to olfactory neurons from endothelial cells by endocytosis or pinocytosis, for final delivery within axons.[15] Among the various nanoparticle types, lipid-based nanoparticles, such as nanoemulsions, solid lipid nanoparticles (SLNs), and nanostructured lipid carriers (NLCs), may be suitable to solubilize poorly water-soluble drugs[16] due to their rapid uptake and biodegradation, low toxicity, absence of a burst release effect, and easy scale-up process.[9] However, there are certain limitations of intranasal administration, such as decreased therapeutic efficacy as a result of the short nasal residence time of the administered drug due to the rapid mucociliary clearance mechanism.[7,9,13] Nonetheless, these challenges can be addressed by in-situ gel (ISG) systems. ISG systems involve stimuli-responsive gelling in physiological nasal conditions.

In this review, we organized the content into four main sections, providing a comprehensive exploration of the drug delivery process from the nose to the brain. The first section explores the basics of administering medicine through the nose, followed by a review of the use of lipid-based nanoparticles and ISGs to improve delivery. The next section discusses the challenges in administering medicine through the nose. Finally, the review discusses the use of the quality by design (QbD) approach and the current market situation.

Nose-to-Brain Drug Delivery Systems

Conventional methods of administering drugs for brain-targeting systems, such as oral and parenteral routes, involve delivering drugs into the brain through the systemic circulation.[7,17] However, the majority of administered drugs often remain in the systemic circulation due to challenges in penetrating physiological barriers, such as the BBB. Specifically, large molecules and more than 98% of low-molecular-weight drugs face difficulties permeating the BBB, resulting in low brain bioavailability.[18] Additionally, oral administration leads to hepatic first-pass metabolism and intestinal enzymatic degradation prior to the arrival of the drug in the brain.[7] Parenteral administration, like intrathecal delivery, can lead to complications, such as cerebrospinal fluid leakage and meningeal issues.[19] On the other hand, the receptor-mediated approach has gained attention as a potentially safe and effective method for enhancing brain-targeting capability without disrupting the BBB membrane.[8,20] However, this strategy carries the risk of losing therapeutic effectiveness due to the accumulation of drug carriers in unintended sites, such as the liver.[15]

In 1989, William H. Frey II introduced intranasal administration as a non-invasive approach for nose-to-brain delivery.[7,21] This approach capitalizes on the direct connection between the olfactory nerve and the frontal region of the brain, facilitated by the olfactory bulb, as well as the entry of the trigeminal nerve through the trigeminal ganglion and pons. These connections provide opportunities for bypassing the BBB, evading hepatic first-pass effects, and preventing intestinal enzyme degradation. Nose-to-brain delivery also boasts high patient compliance and affordability, and it eliminates the need for expert interventions. General information regarding oral, parenteral, and intranasal administration routes is summarized in Table 1.

Anatomy of the Nasal Cavity

The nasal cavity can be divided into the vestibule, atrium, turbinate (respiratory), and olfactory regions. The upper part of the nasopharynx is connected to the nasal cavity.[14] The outermost nasal cavity is the vestibule (0.6 cm^2), which is lined by keratinized and stratified squamous epithelium with embedded vibrissa.[22,23] The vestibule filters foreign substances larger than 10 μm via the mucus layer covering the surface of the vibrissa. The vestibule exhibits low drug permeability

Table 1 Comparing Oral, Parenteral, and Intranasal Administration for Brain-Targeting Systems

	Oral Administration	Parenteral Administration	Intranasal Administration
Patient compliance	High	Low	High
Hepatic first-pass metabolism	Dominant	Avoidable	Avoidable
Intestinal enzymatic degradation	Dominant	Avoidable	Avoidable
Onset of action	Relatively slow	Fast (IV injections) Slow (SC and IM injections)	Fast
BBB penetration	Difficult	Difficult	Avoidable
Dosage form	Tablet and capsule	Injection	Spray

Abbreviations: BBB, blood-brain barrier; IV, intravenous; SC, subcutaneous; IM, intramuscular.

because of the keratinized squamous epithelium.[23] The atrium is the intermediate epithelial section between the vestibule and the turbinate region.[14,22] It also shows low drug permeability as it is the narrowest area and is composed of stratified squamous epithelium.[23] Toward the inner region, the widely spread respiratory region is the most significant part of the nasal cavity (approximately 130 cm^2). The inferior, middle, and superior turbinates are located in the respiratory region.[14] The respiratory region comprises ciliated, goblet, basal, and pseudostratified columnar epithelial; trigeminal nerve (higher); and olfactory nerve (lesser) cells.[13] In this region, the mucus layer, also known as the mucosa, regulates the filtration and humidification of inhaled air.[22,24] The high degree of vascularization and large surface area of the respiratory region facilitate the uptake of most drugs administered to that region, to compared to other nasal cavity regions.[23] Conversely, the olfactory region (10–20 cm^2) is in the uppermost region of the respiratory section.[14,23] The olfactory epithelium comprises microvillar, basal, olfactory nerve (higher), and trigeminal nerve (lesser) cells.[13] The unique anatomical structure of olfactory nerves connecting the olfactory bulb through the cribriform suggests the possibility of direct drug delivery into the brain.

Pathway of Intranasal Transport to the Brain

The motivation for developing intranasal drug administration stems from the challenge of delivering drugs to the brain while overcoming the Blood-Brain Barrier (BBB).[13] Two primary delivery pathways in intranasal administration, the olfactory and trigeminal nerve pathways, provide direct routes to the brain (Figure 1).[7,25] However, not all drugs administered intranasally are confined to these pathways. Some drugs may enter systemic or lymphatic circulations, where crossing the BBB is necessary to reach the brain. In such cases, the quantity of the drug that successfully penetrates the BBB and reaches the brain is often limited.

In the olfactory nerve pathway, olfactory receptors in the olfactory epithelium absorb drugs by endocytosis or passive diffusion and deliver them toward the olfactory nerve axons through intracellular axonal transport.[7,13,21,26] Small-molecule drugs of less than 200 nm are exceptionally acceptable due to the olfactory nerve axon's size.[13] The unique structure of the axons surrounded by the olfactory ensheathing cells extending to the olfactory bulb across the cribriform indicates the possibility to deliver drugs from the peripheral nervous system (the olfactory epithelium) to the CNS (the brain).[27] After drugs reach the lamina propria of the olfactory epithelium by transcellular or paracellular transport mechanisms, they are further delivered to the perineural space filled with cerebrospinal fluid (CSF), which connects the subarachnoid region.[7,13,26,28,29]

In the respiratory system, drugs are transported to the brain via the trigeminal nerve pathway. The trigeminal nerve is the fifth cranial nerve and it is innervated with ophthalmic, maxillary, and mandibular nerve branches, which gather in the trigeminal ganglion.[17,21,30] The trigeminal nerve originates from the pons of the brainstem, allowing it to be a potential target nerve for drug transport to the CNS.[7,12–14,21] In particular, drugs absorbed in the maxillary and ophthalmic nerve branches can be delivered to the brainstem via the pons, allowing the potential for brain-targeted delivery.[21,30,31] The

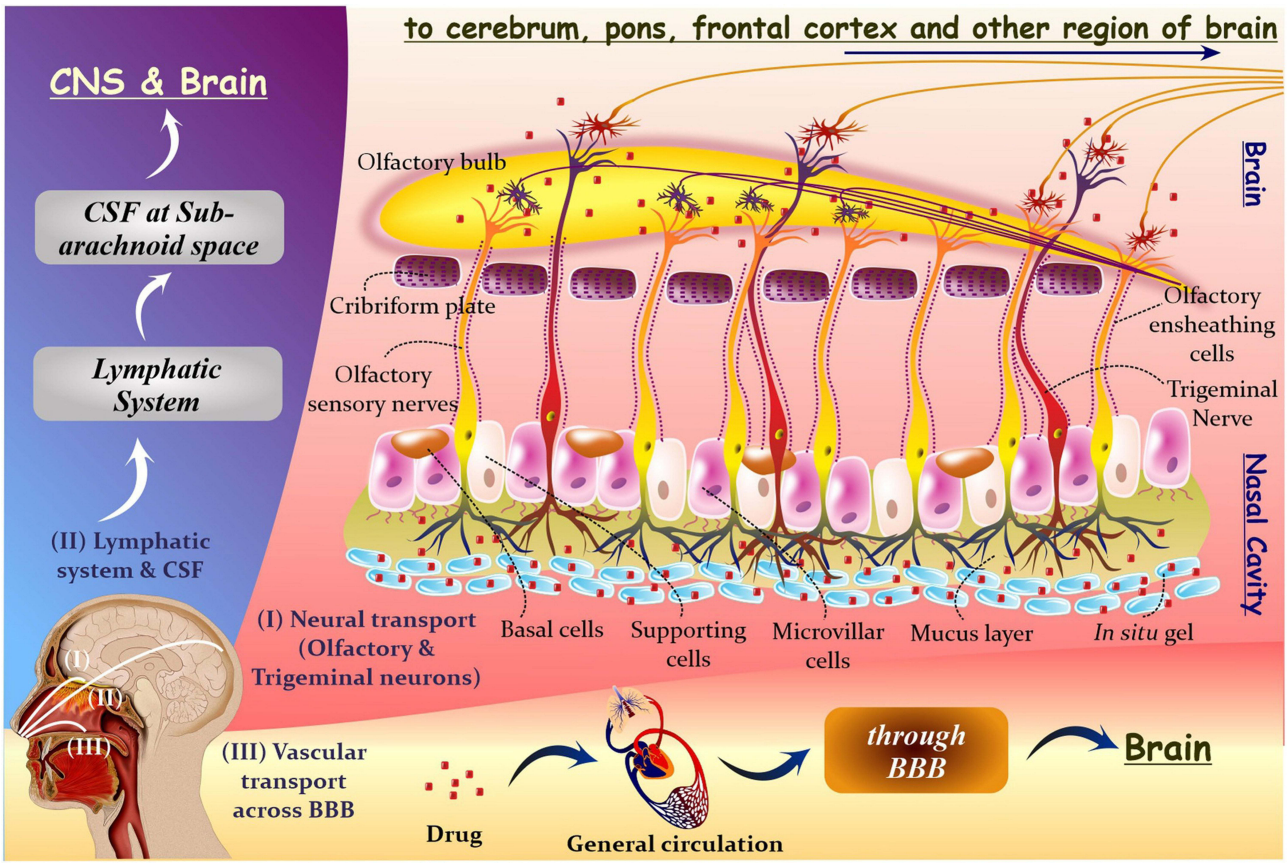

Figure 1 Intranasal mechanism of nose-to-brain delivery. The therapeutics can be transported from the nose to the brain through (I) neural transport through the olfactory and trigeminal nerves, (II) lymphatic system and cerebrospinal fluid (CSF), and (III) vascular transport across the blood-brain barrier (BBB). The primary routes for nose-to-brain are olfactory and trigeminal nerve pathways. In contrast, the latter two serve as secondary passages. Reprinted from *J Cont Rel*, Volume 327, Agrawal M, Saraf S, Saraf S, et al. Stimuli-responsive in situ gelling system for nose-to-brain drug delivery. 235–265. Copyright 2020, with permission from Elsevier.[13]

trigeminal nerve pathway allows nose-to-brain delivery through intracellular axonal transport and extracellular mechanisms, similar to those of the olfactory nerve pathway.[14,32] The trigeminal nerve pathway presents a slower intracellular transportation rate than the olfactory nerve pathway.[26]

Factors Affecting Intranasal Drug Delivery

Effective intranasal drug delivery requires a comprehensive understanding of the anatomy of the nasal cavity and the intranasal drug delivery pathways in the brain. Most evidence for the efficacy of intranasal drug delivery comes from rodent models developed by skilled professionals, but human anatomical features are different from those of rodents. Nonetheless, these animal studies are crucial for optimizing therapeutic development in humans. The representative influencing factors related to intranasal drug delivery were classified in Figure 2 as per biological, physicochemical, and formulation perspectives.

Mucin Secretion

Following intranasal administration, the nasal mucosa acts as the primary barrier for drugs,[18,26] protecting the nasal epithelium against foreign particles and regulating temperature and humidity.[24] The nasal mucosa is covered with mucus, comprising mucin proteins secreted by goblet cells.[31,32] Mucus also contains other substances that have antimicrobial and immunomodulatory effects and can degrade biological entities.[26]

Mucin comprises elongated and flexible domains known as "PTS" domains, which consist of proline, threonine, and serine residues.[23,33] Most of the threonine and serine residues in the PTS domains are linked to glycan molecules. These glycans terminate with negatively charged carboxyl groups containing sialic acid, resulting in a considerable negative

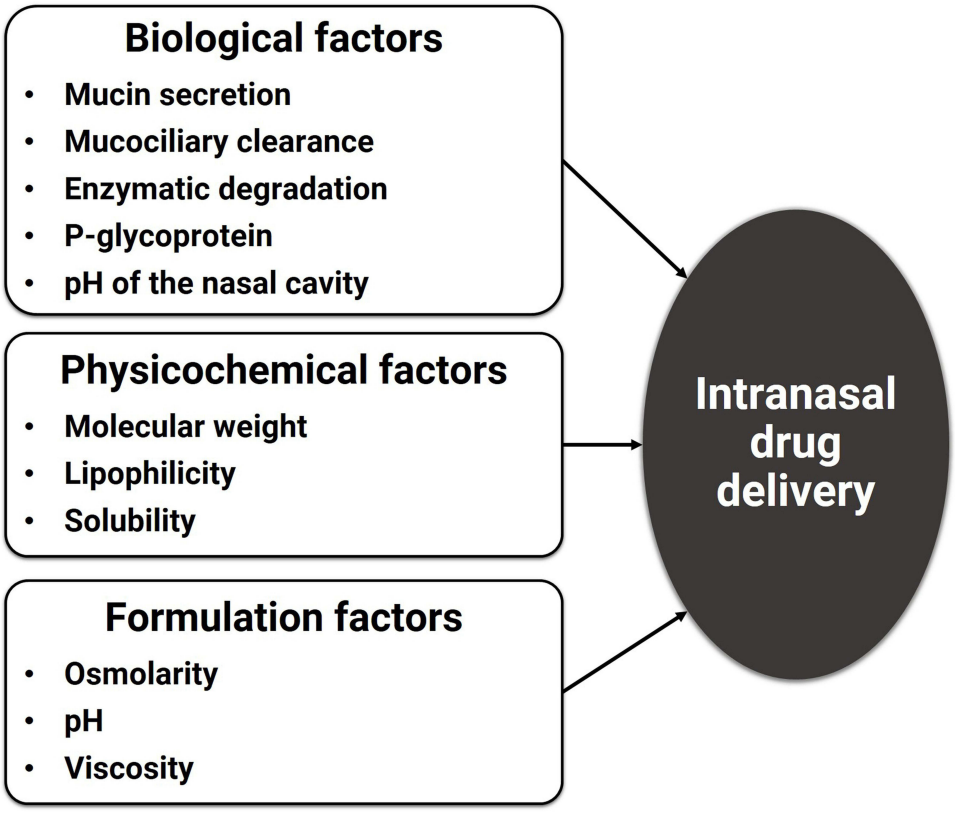

Figure 2 Representative factors influencing intranasal drug delivery. Those factors can be classified depending on the biological environment of the nasal cavity, physicochemical properties of drugs, and characteristics of final formulation or pharmaceutical dosage forms.

charge on the PTS domains. Each mucin monomer has a length of approximately 0.2–0.6 μm and is connected end-to-end with other monomers through disulfide bonds.

High concentrations of Ca^{2+} and H^{+} within the mucin granules result in densely packed long multimeric fibers.[23,26,33] H^{+} neutralizes carboxyl groups, whereas Ca^{2+} crosslinks the remaining glycans before secretion. Following mucin secretion, the diffusion of H^{+} and Ca^{2+} causes entanglement of mucin bundle fibers. These properties have significant implications for mucin-based formulations and drug delivery.

Hydrophobic or charged hydrophilic molecules diffuse poorly through mucus, while uncharged hydrophilic molecules can move quickly through the mucin mesh, with smaller molecules moving almost as fast as water.[26] The thickness of mucus can vary depending on its water content, but nasal mucus is generally thin and not a significant consideration in most clinical cases.

Mucociliary Clearance

Within the nasal mucosa, the movement of ciliated hairs facilitates the removal of inhaled particles captured in the mucus from the nasal cavity to the nasopharynx.[9,32] This process, known as nasal mucociliary clearance, is a self-defense mechanism that prevents harmful substances from entering the nose.[9,32] However, it also affects the retention time of drugs in the nasal mucosa, directly influencing the success of nose-to-brain drug delivery.[14,21] The rate of nasal mucociliary clearance is approximately 10–20 min,[26] and the olfactory region displays a slower rate of mucociliary clearance than the respiratory region.[9]

In general, liquid dosage forms have a shorter residence time in the nasal cavity than powder forms due to mucociliary clearance, because powders tend to adhere to the moist nasal epithelial surfaces.[9]

The secretion and flow of mucin in the intranasal administration route are among the primary challenges hindering drug absorption. Strategies such as adjusting nanoparticle size, balancing hydrophilic and lipophilic properties of particles, and using mucolytic agents have been proposed to overcome these mucin-related limitations.[34,35] However, mucin secretion continues to be a hurdle in drug delivery. The use of intranasal in-situ gel is considered a potential solution to overcome these challenges. The formation of a gel within the nasal cavity increases the viscosity of the

formulation.[13] This, in turn, extends the contact time with the nasal membrane, resulting in increased retention time, which can reduce the rate of drug loss. While this approach may still be influenced by mucociliary clearance, it is relatively more effective in overcoming this limitation and is regarded as an efficient formulation strategy.

Enzymatic Degradation

Although drugs administered to the nasal cavity can avoid gastrointestinal degradation and the hepatic first-pass effect, the nasal cavity contains hydrolytic enzymes as part of its defense mechanism against xenobiotics, leading to enzymatic drug degradation.[9,36] Consequently, this induces a pseudo-first-pass effect that interferes with drug absorption[37] and negatively affects the pharmacokinetic and pharmacodynamic profiles of the drugs.[36]

P-Glycoprotein

The olfactory epithelium has a slower mucociliary clearance time than the respiratory epithelium because of the absence of motile cilia.[9,26] However, the high expression levels of p-glycoprotein pumps in the olfactory epithelia may counteract this effect.[26]

Molecular Weight and Lipophilicity

The absorption of drugs by the nasal epithelium is influenced by their molecular weight and lipophilicity. Drugs with molecular weights less than 300 Da easily cross the nasal epithelium and are rapidly absorbed, irrespective of their lipophilicity.[32,36,37] In contrast, hydrophilic molecules can be absorbed through the mucosal epithelia paracellularly or via carrier-mediated transport, whereas lipophilic molecules are typically absorbed through passive diffusion.[9]

Lipophilicity is particularly relevant for drugs with molecular weights ranging from 300 to 1000 Da.[9,32] Lipophilic drugs pass through passive diffusion, whereas hydrophilic drugs use a paracellular pathway. However, lipophilic high-molecular-weight drugs exhibit reduced absorption.[32,37] Conversely, hydrophilic macromolecules (> 1000 Da), such as proteins and peptides, have very low bioavailability and are absorbed via endocytosis.[9]

Solubility

Drug solubility in the nasal physiological fluid can influence the extent of nasal absorption.[9,32,37] Due to the watery nature of nasal secretions, appropriate aqueous-soluble forms of drugs can remain in molecular dispersion or solution form to enhance their dissolution.[9,37] However, the low nasal cavity volume poses a challenge for drugs with poor aqueous solubility or those administered at high doses.[9] Various strategies to improve drug solubility for nose-to-brain delivery have been studied using prodrugs; salt forms; and the utilization of co-solvents, cyclodextrins (as solubilizing excipients), and nanoparticle systems.

Formulation Factors

The osmolality of nasal formulations is a crucial factor, since hypertonic and hypotonic formulations can disrupt normal cilial movement, leading to reduced nasal drug absorption.[32] Therefore, nasal formulations should ideally be isotonic,[32,37] falling within the acceptable range of 290 to 500 Omol/kg.[36] Commonly used isotonizing excipients include glycerine, sodium chloride, glucose, and dextrose.[32]

The pH of the nasal formulation should be adjusted to a range of 4.5–6.5 to prevent nasal irritation.[37,38] By avoiding irritation, efficient drug permeation can be achieved, and bacterial growth can be prevented.[38]

Enhancing the viscosity of nasal formulations may extend the therapeutic effect by altering ciliary beating and mucociliary clearance, thereby increasing drug permeation.[36,38] However, increasing viscosity may pose a challenge, as it can reduce drug diffusion from the formulation.

Devices for Nasal Administration

The deposition of drugs administered in the nasal epithelium plays a crucial role in influencing the nose-to-brain pathway, making it vital to maximize drug deposition on the olfactory epithelium for successful treatment efficacy.[39–41] Traditional intranasal devices of liquid formulations, such as droppers and spray pumps, face challenges in delivering drugs to the olfactory epithelium because of their location in the upper part of the nose and the restrictions imposed by the nasal turbinate. For example, less than 3% of the drug reaches the olfactory region using a spray pump, and a dropper requires a precise patient position. Consequently, the drug may be absorbed systemically by blood vessels or cleared via

mucociliary clearance. To overcome the disadvantages of conventional devices, researchers have developed devices capable of delivering drugs in different forms (powders or liquids).

Examples of advanced nasal devices used in clinical trials are listed in Table 2. Briefly, ViaNase™, an electronic atomizer device developed by Kurve Technology® (Lynnwood, WA, USA), comprises a nebulizer connected to a vortex chamber.[40] A precision olfactory delivery system developed by Impel NeuroPharma (Seattle, WA, USA) incorporates a tank, compressed air or nitrogen, and a chlorofluorocarbon (or hydrofluoroalkane) aims to deliver drugs to the olfactory region.[41] SipNose (Yokne'am Illit, Israel) pioneered a nasal device triggered by drinking action, permitting aerosol delivery.[40] OptiNose™ (OptiNose, Yardley, PA, USA) is a bi-directional delivery device that requires an exhalation force for the patient to administer.[40]

Strategies to Improve Drug Delivery via the Intranasal Route

Non-Invasive Methods

Two strategies can be used to overcome the BBB: invasive and noninvasive approaches. Invasive techniques involve direct injection into the brain parenchyma or cerebrospinal fluid or the therapeutic opening of the BBB.[42,43] The direct injection of drugs or implantation into the brain parenchyma has been studied to treat neurological and mental disorders and stroke.[42] However, direct injection can be less efficient because of limited diffusion between the cerebrospinal and extracellular fluids. In addition, there are potential risks of brain tissue damage and significant fluctuations in intracranial pressure.[44] The other invasive approach, temporarily opening the BBB, necessitates collaboration with highly trained neurosurgeons and it may cause potential adverse effects from BBB disruption, such as hemorrhage and brain damage or inflammation.[8]

Non-invasive methods utilize endogenous cellular mechanisms to facilitate the transport of drugs into the CNS through the transcellular pathway.[12] Non-invasive strategies include the nose-to-brain route of administration, the inhibition of efflux transporters, the development of prodrugs and chemical drug delivery systems, and the application of nanocarriers.[42] Among these methods, intranasal delivery offers several advantages, such as a large surface area, ease

Table 2 Examples of Advanced Nasal Devices Used in the Clinical Trials

Nasal Device (Type)	Available Dosage Form	Manufacturer	Clinical Trial (Condition/Disease, Phase, Status)
ViaNase (electronic atomiser)	Liquid	Kurve Technology, USA	NCT02988401 (multiple sclerosis, 1/2, C) NCT02810392 (stroke, 2, C) NCT04739371 (insulin, 1, A) NCT03943537 (cognitive diseases, 2, R)
Precision olfactory delivery (semi-disposable unit dose delivery)	Liquid and powder	Impel Pharmaceuticals, USA	NCT03624322 (acute agitation, 1, C) NCT03541356 (Parkinson's disease, 2, C) NCT02758691 (insulin, 1, C) NCT05163717 (agitation, 2, A) NCT03401346 (migraine, 1, C) NCT03557333 (migraine, 3, C)
SipNose (pressurised delivery)	Liquid and powder	Sipnose, Israel	NCT04028960 (type 1 diabetes, 2, T) NCT03901781 (ocular hypertension, 1, C)
OptiNose™ (insufflator)	Liquid and powder	Optinose, USA	NCT01983514 (healthy male adults, 1, C) NCT02414503 (ASD, 1/2, C) NCT02266927 (asthma, 1, C) NCT01507610 (migraine, 1, C) NCT01623310 (nasal polyps, 3, C) NCT01622569 (nasal polyposis, 3, C) NCT01624662 (nasal polyposis, 3, C) NCT01667679 (migraine, 3, C)

Abbreviations: A, active; C, completed; R, recruited; T, terminated; ASD, autism spectrum disorder.

of self-administration, avoidance of hepatic first-pass metabolism, a highly vascular mucosa, and increased absorption.[45] Nanoparticles are attractive agents to facilitate drug transport into the CNS through nose-to-brain delivery, as they can protect the drug from enzymatic degradation and improve its plasma stability and solubility.[42] Furthermore, they can be specifically designed for targeted delivery, thus minimizing non-desired side effects.

Lipid-Based Nanoparticles

Advantages for Intranasal Administration

Lipid-based nanoparticles, which are colloidal systems composed of lipids or oils, surfactants, and other additives, have garnered significant attention as a promising approach for delivering drugs from the nose to the brain.[14,15,46] The popularity of these nanoparticles stems from their improved compatibility with the body, cost-effectiveness, safety, and effectiveness. Encasing drugs within lipid structures facilitates drug absorption through cell membranes.[46] This encapsulation also protects drugs from degradation caused by biological and chemical factors, and prevents them from being transported by efflux proteins.[14,15]

When developing lipid-based nanoparticles for delivering drugs from the nose to the brain, it is crucial to optimize certain factors to ensure successful drug transport into the brain.[12,21,46] These factors include particle size, particle size distribution (PDI), zeta potential, drug loading, release behavior, surface modification, and colloidal stability.[12]

Various reports have suggested that the particle size should generally be less than 200 nm.[21,46] Additionally, the PDI can impact how lipid-based nanoparticles behave in the body, affecting their circulation time, absorption, and distribution.[12] For intranasal formulations, a PDI less than 0.3 is typically recommended, although this can vary depending on the type of lipid-based nanoparticle used.[21] Nanostructured lipid carriers tend to have higher PDI values than nanoemulsions because of the asymmetrical shape of non-spherical lipid nanoparticles.[21] Smaller PDI and particle size values contribute to uniform drug absorption through the nasal mucosa.

Another essential aspect that influences how well a drug performs after intranasal administration is the zeta potential, which indicates the nanoparticle's surface charge and predicts its long-term physical stability.[21] A zeta potential value above or below ±30 mV indicates good stability, reducing the likelihood of nanoparticles merging together. Nanoparticles with positive zeta potentials interact well with negatively charged mucin residues, leading to increased retention of the formulation in the nasal mucosa over an extended period.[12,16,46] However, an excessively high surface charge can potentially induce toxicity.

Certain surfactants, such as PEGylated molecules, can maximize the colloidal stability of nanoformulations and enhance drug permeation. Similarly, mucoadhesive polymers that interact with mucin are employed to prolong nanoparticle residence in the nasal passage.[12] Additionally, incorporating cell-penetrating peptides that interact with cell membranes can promote the uptake of nanoparticles into cells.[12,16]

Nose-to-Brain Delivery Efficiency of Nanoparticles

Since intranasal administration can also lead to systemic drug circulation across the BBB and subsequent delivery of the drug into the brain, it is not feasible to directly measure the extent of nose-to-brain drug delivery.[16,47] However, a reliable estimation can be made by comparing brain uptake after intranasal and intravenous administration. The drug-targeting efficiency (DTE) and direct transport percentage (DTP) metrics have been established to estimate nose-to-brain drug delivery.

DTE % offers a relative cerebral exposure value of drugs after intranasal administration compared to intravenous administration.[16] The area under the curve (AUC) of drug concentration versus time plots in the brain and blood for both routes of administration is used to calculate DTE % according to Equation 1.

$$\mathrm{DTE}\,\% = \frac{AUC(brain, IN)/AUC(blood,\ IN)}{AUC(brain, IV)/AUC(brain, IV)} \times 100 \tag{1}$$

In Equation 1, *AUC(brain)* and *AUC(blood)* denote the AUC values in the brain and blood, respectively. Theoretically, the DTE % value should exceed 100%. A value of 100% indicates no drug transport into the brain across the BBB (AUC(brain, IV) = 0) or no drug absorption into the systemic circulation after intranasal administration *(AUC(blood, IN)* = 0).[47] High DTE values imply substantial drug delivery efficiency through the nose-to-brain route.[16]

DTP % quantifies the percentage of the relative ratio between nose-to-brain drug delivery and all possible brain delivery pathways after intranasal administration.[16] To assess the overall percentage of nose-to-brain delivery, the portion delivered via the BBB can be subtracted from the total brain concentration. Equation 2 explains the method used to calculate the DTP % value.

$$\mathrm{DTP}\,\% = {}^{\mathrm{B(IN\ )\ -\ B(X\ )}}\!/_{\mathrm{B(IN\ )}} \times 100 \tag{2}$$

In Equation 2, *B(IN)* signifies the entire brain AUC following intranasal administration and *B(X)* accounts for the fraction attributed to systemic drug delivery across the BBB.

B(IN) is obtained by directly analyzing drug levels in the brain or cerebrospinal fluid. It is essential to administer intranasal and intravenous routes to the same animal species to calculate *B(X)* using Equation 3, where *B(IV)* is the brain AUC following intravenous administration, while *P(IV)* and *P(IN)* correspond to the plasma AUC after intravenous and intranasal administration, respectively.

$$B(X) = {}^{\mathrm{B(IV\ )}}\!/_{\mathrm{P(IV\ )}} \times P(IN) \tag{3}$$

Preclinic Applications on Nose-to-Brain Delivery

Table 3 outlines the studies that have investigated the application of lipid-based nanoparticle systems for intranasal administration. In this table, the API, excipient, and particle properties of each nanoformulation are presented. In the following section, we discuss the various formulation types applicable to the intranasal route, along with the specific characteristics of each formulation.

Table 3 Information of Optimal Lipid-Based Nanoparticles Investigated Formulations for Nose-to-Brain Delivery

Lipid-Based Nanoparticle			Note	Ref.
Drug (Indication)	**Excipient**	**Particle Properties**		
Nanoemulsion				
Insulin (diabetes mellitus)	Capmul MCM, Captex 8000, Cremophor RH40,	PS 32.2 nm and PDI 0.250	• Self-nano emulsifying drug delivery system (SNEDDS) was researched. • The emulsion (IN) showed the highest glucose reduction level and AUC.	[48]
Huperzine A (AD)	Isopropyl myristate, Capryol 90, Cremophor EL, and Labrasol	PS 15.24 nm, PDI 0.128, and ZP −4.48 mV	• Lactoferrin was modulated to enhance the brain-targeted efficiency through receptor-mediated transcytosis. • The DTE of the nanoemulsion (IN) was 320%.	[49]
Donepezil (AD)	Labrasol, cetylpyridinium chloride, and glycerol	PS 65.36 nm, PDI 0.084, ZP −10.7 mV	• The DTE and DTP values of the nanoemulsion (IN) as 360.59% and 72.23% confirmed a facilitated drug delivery through the N2B route.	[50]
Gabapentin (epilepsy)	Capmul MCM, Tween 80, PEG 400, and Carbopol 934	PS 43.76 nm, PDI 0.525, and ZP −13.95 mV	• The Carbopol 934 improved viscosity and retention time on the nasal mucosa tissue while increasing the particle size. • PEG 400 enhanced the ex-vivo permeation rate.	[51]
Tetrabenazine (HD)	Capmul MCM, Tween 80, and Transcutol P	PS 106.80 nm, PDI 0.198, and ZP −9.63 mV	• The nanoemulsion (IN) demonstrated higher and lower drug concentrations in the brain and plasma, respectively, compared to the free drug solution (IV).	[52]
Bromocriptine mesylate and glutathione (PD)	Capmul PG-8 NF, PEG 400, and propylene glycol	PS 80.71 nm, PDI 0.217, and ZP −12.60 mV	• The nanoemulsion (IN) enhanced in-vivo behaviors on forced swimming, locomotor activity, catalepsy, rota-rod, and akinesia.	[53]
Naringenin (PD)	Capryol 90, vitamin E, Tween 80, and Tanscutol HP	PS 38.70 nm, PDI 0.14, and ZP −27.4 mV	• The nanoemulsion (IN) illustrated higher DTE and DTP values (823% and 72%) than the free drug solution (IN) (667% and 68%).	[54]

(*Continued*)

Table 3 (Continued).

Lipid-Based Nanoparticle			Note	Ref.
Drug (Indication)	**Excipient**	**Particle Properties**		
Luteolin (neuroblastoma)	Oleic acid, ethylene glycol, Tween 20, and chitosan	PS 68 nm, PDI, ZP +13 mV, and EE 85.5%	• The chitosan was mixed into the aqueous phase as a mucoadhesive agent. • The nanoemulsion (IN) prolonged a drug half-life in the brain and induced apoptosis on the blastoma cell.	[55]
Ronic acid (Neuronal disease)	Medium chain triglyceride, Lipoid E80, and chitosan	PS 258.01 nm, PDI 0.22, and ZP 44.98 mV	• The viscosity and mucoadhesive force increased after the chitosan application into the nanoemulsion. • The chitosan addition also prolonged the retention time on the nasal mucosa.	[56]
6-Gingerol (ischemia)	Lauroglycol 90, Tween 80, PEG 400, and chitosan	PS 94.89 nm, PDI 0.129, and ZP +1.892 mV	• The chitosan was applied to improve the mucoadhesive property. • The nanoemulsion (IN) reduced tissue damage and improved in-vivo neurobehaviors significantly comparing to the free drug solution (IN).	[57]
Topiramate (epilepsy)	Capmul MCM C8, Tween 20, and Carbitol	PS 4.73 nm, PDI 0.206, and ZP +10.74 mV	• The nanoemulsion (IN) significantly reduced the epileptic seizure duration and presented the highest drug level in the brain.	[58]
Memantine (AD)	Labrasol, cetyl pyridinium chloride, and ethylene glycol	PS 11 nm, PDI 0.08, and ZP −19.6 mV	• The nanoemulsion (IN) successfully delivered drugs into the brain via systemic and N2B routes, showing DTE and DTP as 158.78% and 37.05%.	[59]
Letrozole (epilepsy)	Triacetin, Tween 80, and PEG 400	PS 95.59 nm, PDI 0.62, and ZP −7.12 mV	• The nanoemulsion (IN) delayed the onset time of epileptic seizure, reduced seizure score, and alleviated the occurrence of status epilepticus.	[60]
Vinpocetine (AD)	Oleic acid, polyethylene glycol lithium dodecyl stearate, Transcutol P, and borneol	PS 60.19–71.02 nm and PDI 0.19–0.23	• The borneol was utilised to increase drug distribution into the brain. • The nanoemulsion (IN) at a 1 mg/kg borneol dose allowed the highest drug deposition in the brain.	[61]
β-Caryopyllene (epilepsy)	Soybean lecithin and oleylamine	PS 244.03 n, PDI 0.18, and ZP +41.1 mV	• In the pentylenetetrazole-induced seizure model, the nanoemulsion (IN) delayed the onset of epileptic seizure compared to the control; the free drug (IN) did not show an anti-epileptic effect.	[62]
Liposome				
-	DOPC, CL, and DSPE-PEG	PS 89.7 nm, PDI 0.256, and ZP −18.8 mV	• The neutral PEGylated liposome (IN) showed a higher in-vivo brain-targeting ability than the charged and non-PEGylated liposomes (IN).	[63]
Ghrelin (cachexia)	Soybean PC, DSPE-PEG, CL, and chitosan	PS 72.25 nm, PDI 0.30, ZP +50.30 mV, and EE 53.20%	• The chitosan-coated liposome displayed higher permeation and bioadhesive properties. • The high-pressure homogenization method exhibited a more desirable hydration process than the extrusion.	[64]
Pralidoxime chloride (model drug)	PC and DHDHDAB	PS 80 nm, PDI 0.2, and ZP +6 mV	• The liposome surface was modified with the cationic surfactant DHDHDAB. • The liposome (IN) more inhibited the acetylcholinesterase activity.	[65]
Propyl gallate and lomustine (GBM)	PC and CL	PS 127 nm, PDI 0.142, ZP −34 mV, and EE 63.57% (propyl gallate) and 73.45% (lomustine)	• The co-encapsulation of propyl gallate and lomustine was investigated.	[66]
Propyl gallate (GBM)	PC, CL, and hyaluronic acid	PS 167.9 nm, PDI 0.129, ZP −33.6 mV, and EE 90%	• The propyl gallate-loaded liposome (IN) was coated with hyaluronic acid to improve its stability.	[67]
Imatinib mesylate (AD)	Egg PC, LPC, and CL	PS 102.5 nm, PDI 0.28, and ZP −23 mV	• The liposome formulated with Egg PC and LPC presented a higher drug loading percentage than DOTAP- and LPC-based liposomes. • The liposome (IN) exhibited a sustained drug release into the brain.	[68]

(*Continued*)

Table 3 (Continued).

Lipid-Based Nanoparticle			Note	Ref.
Drug (Indication)	**Excipient**	**Particle Properties**		
Ethylacetate fraction (ischaemic stroke)	PC and CL	PS 204.93 nm, PDI 0.297, ZP −20.8 mV, and EE 88.02%	• In the thin-film hydration method, the increasing PC concentration (70%) with decreasing cholesterol level (30%) improved the film formation. • A higher PC concentration of over 70% induced film breakage. • Even with ten times less drug, liposome (IN) showed similar improvements in the in-vivo animal behavioral functions as a free drug (IN).	[69]
Valproic acid (epilepsy)	PC and CL	PS 92.01 nm, PDI 0.21, ZP −43.47 mV, and EE 85.50%	• Higher cholesterol decreased EE, probably due to the salting-out effect. While increasing PC level improved homogeneity and reduced collision between liposomes. • The liposome (IN) increased the drug elimination half-life in the brain.	[70]
Verapamil (chronic rhinosinusitis)	DOTAP, DSPE-PEG, and CL	PS 115 nm, PDI 0.32, ZP +30 mV, and EE 70%	• PEGylated liposome (IN) overcame nasal mucociliary clearance and improved localized dose availability.	[71]
Solid lipid nanoparticle (SLN)				
Dopamine hydrochloride (PD)	Gelucire 50/13, Tween 85, and glycol chitosan	PS 147 nm, PDI 0.5, ZP +5.222 mV, and EE 81%	• Gelucire 50/13, a PEG-ester mixture, could improve physical storage stability and reduce cytotoxicity towards olfactory ensheathing cells.	[72]
Pueraria flavones (neuronal disease)	Lipoid E80, stearic acid (SA), and borneol (Bo)	PS 154.2 nm, PDI 0.12, and ZP −41.5 mV	• Bo-conjugated SA was employed to increase permeability through the nasal mucosa. • The liposome containing Bo-conjugated SA (IN) increased the brain/blood AUC ratio and confirmed a high brain-targeting ability.	[73]
Naloxone (opioid overdose)	GMS, Pluronic F127, and Tween 80	PS 190.2 nm, PDI 0.082, ZP −16 mV, EE 95.32%	• The drug was encapsulated within the lipid matrix in an amorphous state. • The SLN (IN) delivered a high amount of drug into the brain and decreased transportation into the liver.	[74]
Retinoic acid and *Toxoplasma* lysate antigen (toxoplasmosis)	Compritol, stearyl amine, CL, and PVA	PS 326 nm, PDI 0.27, ZP +47 mV, and EE 89.1% (retinoic acid)	• The antigen was encapsulated as an adjuvant. • The SLN (IN) exhibited superior in-vivo parasitological inhibition and antibody production.	[75]
Rivastigmine tartrate (AD)	GMS and Tween 80	PA 110.2 nm, PDI 0.309, ZP −28 mV, and EE 82.56%	• The SLN (IN) exhibited rapid drug transport into the brain and the highest drug concentration ratio in brain/plasma than drug solution.	[76]
Donepezil hydrochloride (AD)	GMS, Tween 80, and Poloxamer 188	PS 121 nm, PDI 0.194, ZP −24.1 mV, and EE 67.95%	• DTE of 553.95% and DTP of 81.94% for the SLN (IN) indicated a superior brain-targeting ability through the N2B route than the free drug solution (IN).	[77]
Zolmitiptan (migraine)	GMS, soya lecithin, and Pluronic F68	PS 170.34 nm, PDI 0.510, ZP −24.83 mV, and EE 84.17%	• Due to the different drug permeation pathways, the SLN (IN) illustrated higher AUC and Cmax in the brain than the marketed nasal spray (IN).	[78]
Haloperidol (SCZ)	Glyceryl behenate and Tween 80	PS 103 nm, PDI 0.190, ZP −23.5 and EE 79.46%	• The SLN (IN) depicted higher DTE and DTP values (539.31% and 87.22%, respectively) than the free drug solution (IN)	[79]
Buspirone (GAD)	Compritol 888 ATO, Tween 80, and Poloxamer 188	PS 218.60 nm, PDI 0.305, ZP −26.47 mV, and EE 70.13%	• The SLN facilitated the dye uptake and reduced the mucociliary clearance comparing the free dye solution. • DTE and DTP values of the SLN (IN) were 882.59% and 88.67%, respectively.	[80]
Dopamine and grape seed extract (PD)	Gelucire 50/13 and Tween 85	PS 184 nm, PDI 0.32, ZP −2.7 mV, and EE 14% (dopamine) and 54% (grape seed extract)	• The SLN exhibited rapid release of GSE and sustained dopamine release. • The developed SLN formulation was not cytotoxic to olfactory ensheathing and neuroblastoma cells.	[81]

(*Continued*)

Table 3 (Continued).

Lipid-Based Nanoparticle			Note	Ref.
Drug (Indication)	**Excipient**	**Particle Properties**		
Nanostructured lipid carrier (NLC)				
Diazepam (epilepsy)	**Cationic NLC**. Precirol ATO 5, Cetiol V, and stearyl amine	PS 124.40 nm, PDI 0.17, ZP +32.60 mV, and EE 95.76%	• The cationic NLC induced a higher cytotoxicity effect than the anionic NLC.	[82]
	Anionic NLC. Precirol ATO 5, Cetiol V, Tween 80, and SDC	PS 69.59 nm, PDI 0.17, ZP −18.60 mV, and EE 94.96%		
Clozapine (SCZ)	Precirol ATO 5, oleic acid, and Tween 80	PS 178 nm and EE 77.4%	• The NLC (IN) demonstrated a superior drug concentration in the brain than the marketed tablet (PO).	[83]
Sumatriptan (migraine)	Stearic acid, triolein, Brij 35, Briji 72, and CL	PS 101 nm, PDI 0.27, ZP −32 mV, and EE 91%	• The NLC presented in-vitro sustained release. • The NLC (IN) displayed a higher drug concentration ratio of brain/plasma for four hours than the free drug solution (IN).	[84]
Phenytoin sodium (epilepsy)	CL, oleic acid, and Poloxamer 188	PS 32.59/80/124.56 nm, PDI 0.289/0.256/0.303, ZP −16.5~-28.0 mV, and EE 91.17/87.70/81.35%	• Different NLC size ranges (< 50, 50–100, and 100 nm <) were investigated in in-vitro dissolution, ex-vivo permeation, and in-vivo pharmacokinetics. • The small NLC (<50 nm) could deliver the drug faster into the brain than a large particle (100 nm <) due to easy access through the small gap between the olfactory cells to reach the lamina propia region.	[85]
Astaxanthin (neuronal disease)	Precirol ATO 5, vitamin E, Tween 80, SDC, BAC, and glycerin	PS 97.610 nm, PDI 0.294, ZP −23.3 mV, and EE 98%	• The NLC formulation presented a greater neuroprotective effect than the SLN type.	[86]

Abbreviations: DTE, Drug-Targeting Efficiency; DTP, Drug Transport Percentage; EE, Encapsulation Efficiency; in, Intranasal Administration; IV, Intravenous Injection; PDI, Polydispersity Index; PO, Oral Administration; PS, Particle Size; ZP, Zeta Potential; indications; AD, Alzheimer's disease; GAD, generalised anxiety disorder; GBM, glioblastoma multiforme; HD, Huntington's disease; PD Parkinson's disease; SCZ, schizophrenia; Excipients; BAC, benzalkonium chloride; CL, cholesterol; DHDHDAB, dihexadecylmethylhydroxyethylammonium bromide; DOPC, dipalmitoylphosphatidylcholine; DOTAP, 1.2-Dioleoyl-3-trimethylammonium propane; DSPE, 1.2-distearoyl-sn-glycero-3-phosphoethanolamine; GMS, glycerol monostearate; LPC, lysophosphatidylcholine; PC, phosphatidylcholine; PEG, polyethene glycol; SDC, sodium deoxycholate.

Nanoemulsions

Emulsions are colloidal liquid dispersions that consist of two immiscible phases (oil and water), supported by a surfactant if necessary.[47] Nanoemulsions are thermodynamically unstable but kinetically stable.[87] Their larger surface area and higher free energy enable them to remain stable against sedimentation, flocculation, coalescence, and creaming.[87] Commonly utilized oils in the nanoemulsions encompass coconut oil, cottonseed oil, safflower oil, sesame oil, and soybean oil, often blended in varying proportions.[62] The oil selection can directly impact the bioavailable fraction of the active component. Surfactants, characterized by their amphiphilic nature, play a pivotal role in stabilizing nanoemulsions by reducing interfacial tension and preventing droplet aggregation.[62] Examples of surfactants are sodium deoxycholate, Cremophor® EL, Tween® (polyoxyethylene sorbitan monolaurate), Span® (sorbitan monolaurate), Solutol® HS 15 (polyoxyethylene-660-hydroxystearate), Poloxamer®, and sodium dodecyl sulfate.[62] The choice of a surfactant not only influences the size and stability of the nanoemulsion but also affects its toxicity, pharmacokinetics, and pharmacodynamics.[62] In nose-to-brain delivery systems, nanoemulsions can overcome the limitations of drugs, such as poor bioavailability and water insolubility.[87,88] In addition, their lipophilic nature and small particle size enhance uptake across the nasal mucosa, protecting the encapsulated drugs from biological and chemical degradation.[50]

To achieve a more advanced brain-targeted delivery system, surface modification strategies have been investigated. To treat Alzheimer's disease using Huperzine A, Jiang et al modified the surface of nanoemulsions with lactoferrin, a natural cationic glycoprotein (molecular weight of 80 kDa), whose receptors are distributed in respiratory epithelial cells, brain endothelial cells, and neurons.[49] Notably, lactoferrin receptors are upregulated in the CNS of individuals with age-related neurodegenerative diseases. After intranasal administration, the optimal lactoferrin-modified nanoemulsion exhibited a higher drug concentration in the brain than the unmodified nanoemulsion and the free drug solution. Additionally, in-vivo distribution analysis of rat brains

following intranasal administration revealed a higher fluorescence intensity in lactoferrin-modified nanoemulsions than in non-modified nanoemulsions because of the greater affinity for lactoferrin-expressing cells and transcytosis. Another case of modifying the nanoemulsion surface was documented using borneol, a traditional Chinese medicine that enhances the efficiency of drug transport into the brain, cortex, and hippocampus.[61] The authors encapsulated vinpocetine into the borneol-modified nanoemulsion to treat Alzheimer's disease and demonstrated a higher drug concentration in the brain after intranasal administration than the non-modified nanoemulsion.

The modulation of the continuous phase can also positively affect brain-targeted delivery systems. Fachel et al coated a nanoemulsion with a chitosan-containing continuous (water) phase to improve the nasal retention time and performed ex-vivo characterizations.[56] A higher viscosity and mucoadhesive force were observed for chitosan-coated nanoemulsions compared to non-coated nanoemulsions, owing to the well-known enhancing effect of chitosan on the mucoadhesive profile. Similarly, Ahmad et al studied a mucoadhesive nanoemulsion to treat cerebral ischemia by adding chitosan into a continuous phase.[57] The chitosan-modified nanoemulsion exhibited higher viscosity and mucoadhesive strength than the non-modified nanoemulsion because the electrostatic interaction between chitosan molecules and mucus prolonged the nasal residence time. Therefore, intranasal administration of chitosan-modified nanoemulsions resulted in a higher drug concentration in the brain than administration of the free drug solution and positively affected in-vivo neurobehaviors.

Liposomes

Liposomes are small vesicles and comprise amphiphilic phospholipids with hydrophilic heads and hydrophobic tails connected by linkages.[89] They closely resemble biological cellular membranes and can encapsulate hydrophilic drugs in their aqueous core and lipophilic drugs within their lipid membrane.[14,42,90,91] Commonly utilized phospholipids include phosphatidylcholine, phosphatidylethanolamine, phosphatidylserine, phosphatidylinositol, phosphatidic acid, and phosphatidylglycerol.[92] The hydrophilic head can be cationic, neutral, or anionic.[89] In particular, the cationic head facilitates cell incorporation and lysosomal escape through the proton sponge effect, although it may induce cytotoxicity.[89] Simultaneously, the hydrophobic tail influences the volume of the hydrophobic cavity and the ratio between hydrophobic and hydrophilic parts of liposomes.[89] Previous studies have shown that phospholipids can be incorporated into the nasal mucosal membrane by creating new pores in paracellular tight junctions.[14] Cholesterol contributes to increased packaging of phospholipid molecules, reduced aggregation, and enhanced rigidity.[93] Typical linkages between the hydrophilic and hydrophobic parts involve ester, ether, amide, and disulfide bonds.[89] Notably, the disulfide bond can selectively degrade and release pharmaceutic agents with a high glutathione concentration in tumor cells.[89] Furthermore, the PEGylated liposomes can prevent a mononuclear phagocyte system that induces a rapid clearance of liposomes in blood-drug concentration.[89] Surface modifications, such as PEGylation, have also been widely applied to improve brain-targeting efficiency after intranasal administration.

Kurano et al investigated the effects of surface charge and PEGylation on brain-targeted delivery kinetics after intranasal administration, using in-vivo ATTO-DOPE fluorescence imaging and [3H]-cholesterol radioactivity tests (Figure 3).[63] They fabricated liposomes to possess negative, neutral (with and without PEGylation), and positive surface charges with particle sizes of 80–90 nm and PDI values of 0.22–0.26. Although the positive and negative liposomes exhibited strong fluorescence intensity in the olfactory bulb and no significant intensity localization, the non-PEGylated neutral liposomes displayed greater migration into the brain via the olfactory and trigeminal nerve pathways. However, the PEGylated neutral liposomes showed more substantial radioactivity in the brain than the non-PEGylated form because PEG modification confers steric stabilization to nanoparticles within the perivascular and perineural spaces in the brain and increases the extracellular transportation of nanoparticles. These results indicate that the surface charge and PEGylation strongly affect nose-to-brain delivery efficiency.

Similarly, Taha et al developed a PEGylated liposome encapsulating verapamil to overcome nasal mucociliary clearance and thus, decrease drug resistance in the nasal cavity.[71] The PEGylated liposome displayed statistically improved uptake and retention time after intranasal administration compared to administration of the free drug solution, using a human organotypic nasal explant under simulated mucociliary clearance conditions. In addition, the verapamil level in mouse nasal tissue was higher after intranasal administration of the PEGylated liposomes than the free drug solution, because the flexibility of the hydrophilic PEG chain allowed the liposomes to diffuse across the nasal mucus membrane.

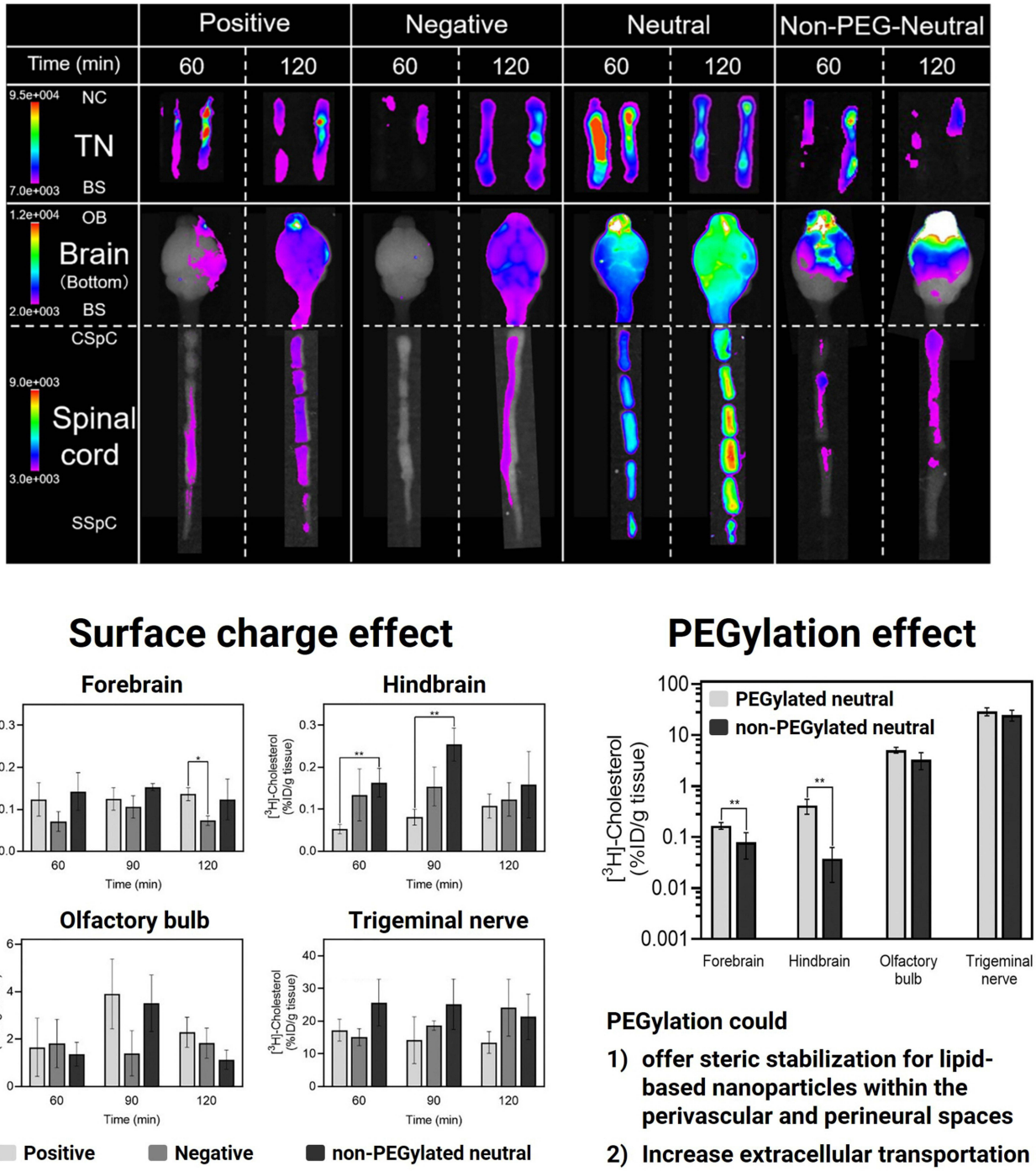

Figure 3 Surface charge and PEGylation effects on nose-to-brain delivery. In-vivo liposome distribution and the surface charge effect on the distribution after intranasal administration were investigated through fluorescence and [^{3}H]-cholesterol radioactivity analysis. The statistical analysis of the surface charge effect was assessed through one-way ANOVA analysis, followed by Tukey's post hoc test (*P < 0.05 and **P < 0.01). Conversely, the Student's *t*-test was performed for the PEGylation effect (**P < 0.01). Reprinted from *J Cont Rel.* Volume 344, Kurano T, Kanazawa T, Ooba A, et al. Nose-to-brain/spinal cord delivery kinetics of liposomes with different surface properties. 225–234. Copyright 2022, with permission from Elsevier.[63]

Abbreviations: TN, trigeminal nerve; NC, nasal cavity; BS, brainstem; OB, olfactory bulb; CSpC, cervical spinal cord; SSpC, sacral spinal cord.

Solid Lipid Nanoparticles and Nanostructured Lipid Carriers

Solid lipid nanoparticles (SLNs) and nanostructured lipid carriers (NLCs) are sub-types of lipid nanoparticles and encapsulate drugs in an organized inner lipid matrix.[14,21,32,46,94] The first generation of lipid nanoparticles, known as SLNs, featured an internally organized matrix primarily composed of lipids.[32] SLN had been explored as an alternative

nanocarrier to liposomes, emulsions, and polymeric nanoparticles by the three research teams of Müller, Gasco, and Westesen in the early 1990s.[95] SLNs are prepared with lipids (glycerol esters, waxes, or fatty acids), emulsifiers (phospholipids, steroids, or non-ionic surfactants), and co-surfactants (anionic surfactants, alcohols, or bile salts).[95] The higher emulsifier concentration decreases the particle size, while the SLN possessing a larger size and broader PDI can be obtained at high lipid levels.[95] The heterogeneous lipid phase comprising miscellaneous lipids could enhance the encapsulation capacity.[95] SLN could enhance the solubility of inadequately water-soluble drugs and can be produced by a straightforward and scalable manufacturing procedure.[14] Nonetheless, specific challenges persisted, encompassing limited encapsulation capacity, drug instability during storage, and the phenomenon of burst release.[14,17,32] Consequently, NLCs have emerged as second-generation lipid nanoparticles. The innovation behind NLCs involves the creation of an internally disorganized matrix using a combination of lipids and oils, resulting in the formation of a less/no crystalline matrix and increased encapsulation efficiency.[96] In detail, the morphological properties of NLC could be summarized into three types: imperfect crystal core for Type I, amorphous lipid matrix for Type II, and tiny oil droplets in fat in water (O/F/W model) for Type III.[96] Cetyl palmitate, glyceryl behenate, glyceryl monostearate, stearic acid, tristearin, and tripalmitin have been extensively employed as lipids.[97] In contrast, caprylic/capric triglycerides and oleic acid are the most commonly utilized oils.[97] Arora et al studied rivastigmine-tartrate-loaded SLNs to treat Alzheimer's disease by intranasal administration.[76] They found the transition of drug molecules into the amorphous state within the SLNs and good compatibility between the drug and lipid matrix by differential scanning calorimetry (DSC) and Fourier-transform infrared (FT-IR) spectroscopy analysis. The melting point of the drug molecule disappeared for the optimized SLNs, as indicated by DSC, and the FT-IR spectra confirmed that there was no interaction between the drug molecules and other excipients. The optimized SLNs depicted no visible damage to the nasal membrane and demonstrated a higher brain-blood ratio in 0.1–8 h than the control solution after intranasal administration. In another study, Yair et al fabricated buspirone-loaded SLNs to overcome the highly variable half-life (2–11 h) and extensive first-pass metabolism of buspirone.[80] The optimized buspirone-loaded SLNs exhibited an absence of drug peaks in the DSC thermogram and X-ray diffraction (XRD) diffractogram, implying possible amorphization of the drug molecules in the lipid matrix. A comparison of the pharmacokinetic profiles of intranasal administration of the optimized formulation and intravenous administration of the drug solution revealed that a considerable amount of the drug reached the brain after intranasal administration, and this was associated with lower plasma drug levels.

Nair et al explored the effect of NLC particle size on the in-vivo pharmacokinetic profiles in the brain, plasma, and CSF after intranasal administration of phenytoin-sodium-loaded NLCs (Figure 4).[85] Two NLCs with different particle size ranges were formulated (< 50 nm and > 100 nm) and their nose-to-brain delivery kinetics were compared. Significant variations in the brain AUC values were evident depending on the particle size following intranasal administration. NLCs < 50 nm exhibited higher AUC values in both the brain and CSF than NLCs > 100 nm, because the smaller NLCs were better able to move through the narrower spaces between olfactory cells, facilitating their passage to the lamina propria region of the olfactory mucosa. This extracellular or extraneuronal mechanism directly promotes drug transport toward the brain parenchymal tissue and CSF. In the olfactory nerve pathway, therapeutic agents absorbed from the olfactory epithelium diffuse through the CSF surrounding the brain via perineural channels.

Comparison Among Nanocarriers

In order to enhance drug delivery efficiency, finding the optimal formulation for intranasal administration is crucial. To determine how much of a drug can be delivered to the brain via the intranasal route, we compare DTE - A relative drug level in the brain after intranasal administration compared to intravenous administration - and DTP - The percentage of the relative ratio between nose-to-brain drug delivery and all possible brain delivery pathways after intranasal administration. This comparison reveals the unique characteristics and delivery efficiency of each formulation.

Pires et al have compared drug delivery efficiencies of various formulations based on data from multiple published nanosystem studies.[47] They found that when drugs are administered intranasally, the use of nanoformulations significantly increases DTE and DTP values compared to when drugs are in solution form, demonstrating the advantages of nanoformulations in intranasal administration.

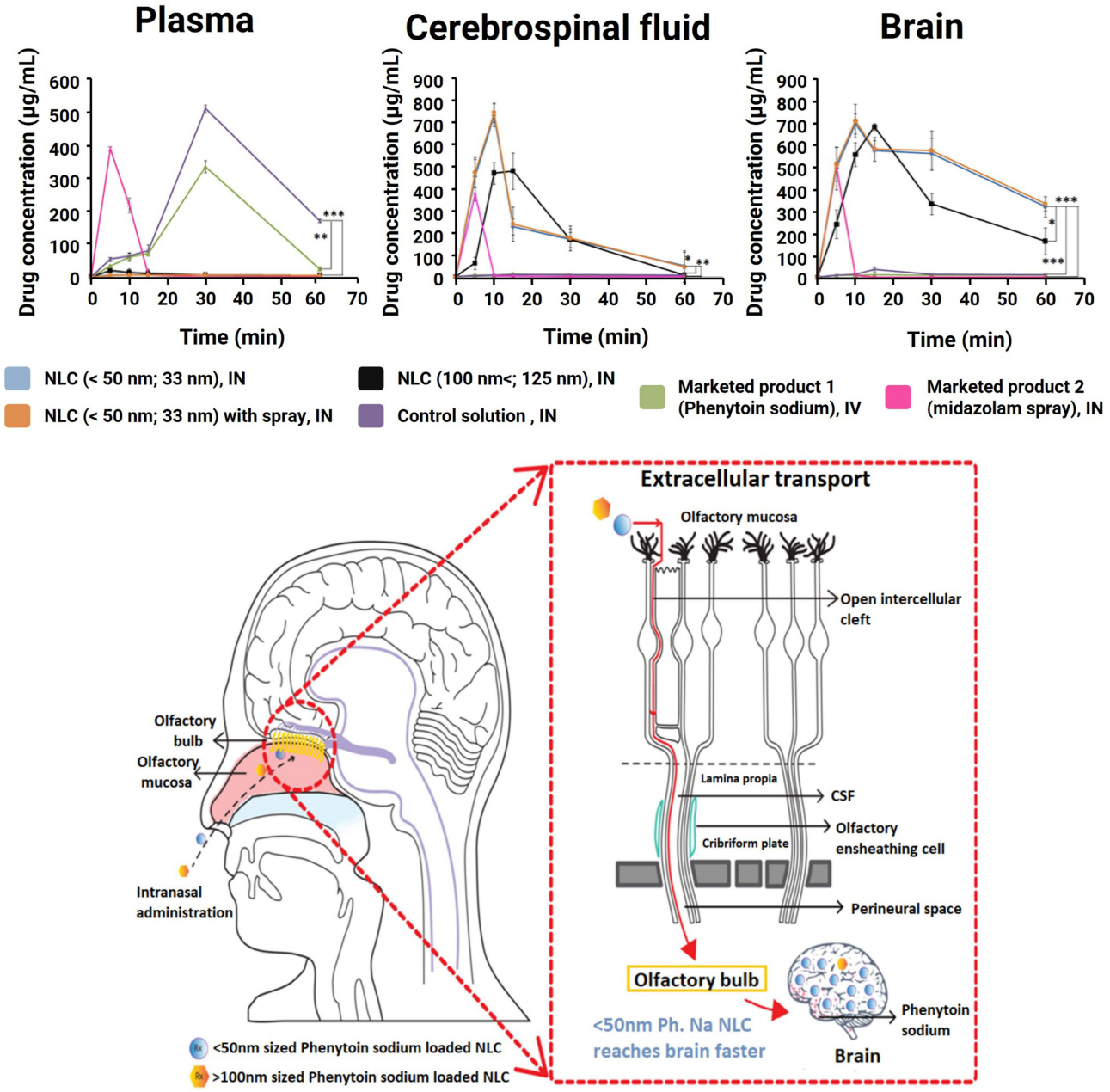

Figure 4 Effect of NLC particle size on nose-to-brain delivery. Drug levels in the plasma, cerebrospinal fluid, and brain after administering NLCs (< 50 nm; 33 nm) by IN, NLCs (< 50 nm; 33 nm) by IN, NLCs (> 100 nm; 125 nm) by IN, a free drug control solution by IN, a commercial product of phenytoin sodium by IV, and another commercial midazolam nasal spray product. The author found that the small NLCs had the most and fastest nose-to-brain delivery transportation of the formulations tested. The statistical significance was evaluated through one-way ANOVA analysis (*p < 0.05, **p < 0.01, and ***p < 0.001). Reprinted from Nair SC, Vinayan KP, Mangalathillam S. Nose to brain delivery of phenytoin sodium loaded nano lipid carriers: formulation, drug release, permeation and in vivo pharmacokinetic studies. Pharmaceutics. 2021;13 (10):1640. Creative Commons.[85]

Abbreviations: CSF, cerebrospinal fluid; IN, intranasal administration; IV, intravenous administration; NLC, nanostructured lipid carrier.

Additionally, when comparing different formulations, polymeric micelle systems showed the highest DTE values.[47] Microemulsions, while having slightly lower DTE and DTP values, were still significantly more efficient than drug solution formulations. However, formulations like liposomes showed very low values. Due to the limited number of studies and only two sources available for calculation, further discussion on these formulations is omitted. This comparative research overall implies that the use of nanosystems for drug delivery to the brain is more efficient than drug solutions, with polymeric micelle systems potentially being slightly superior. However,

it's important to note that these findings are based on data aggregated from various published papers, and differences in the drugs used, frequency of administration, and experimental designs make direct comparison challenging and not entirely conclusive (Figure 5).

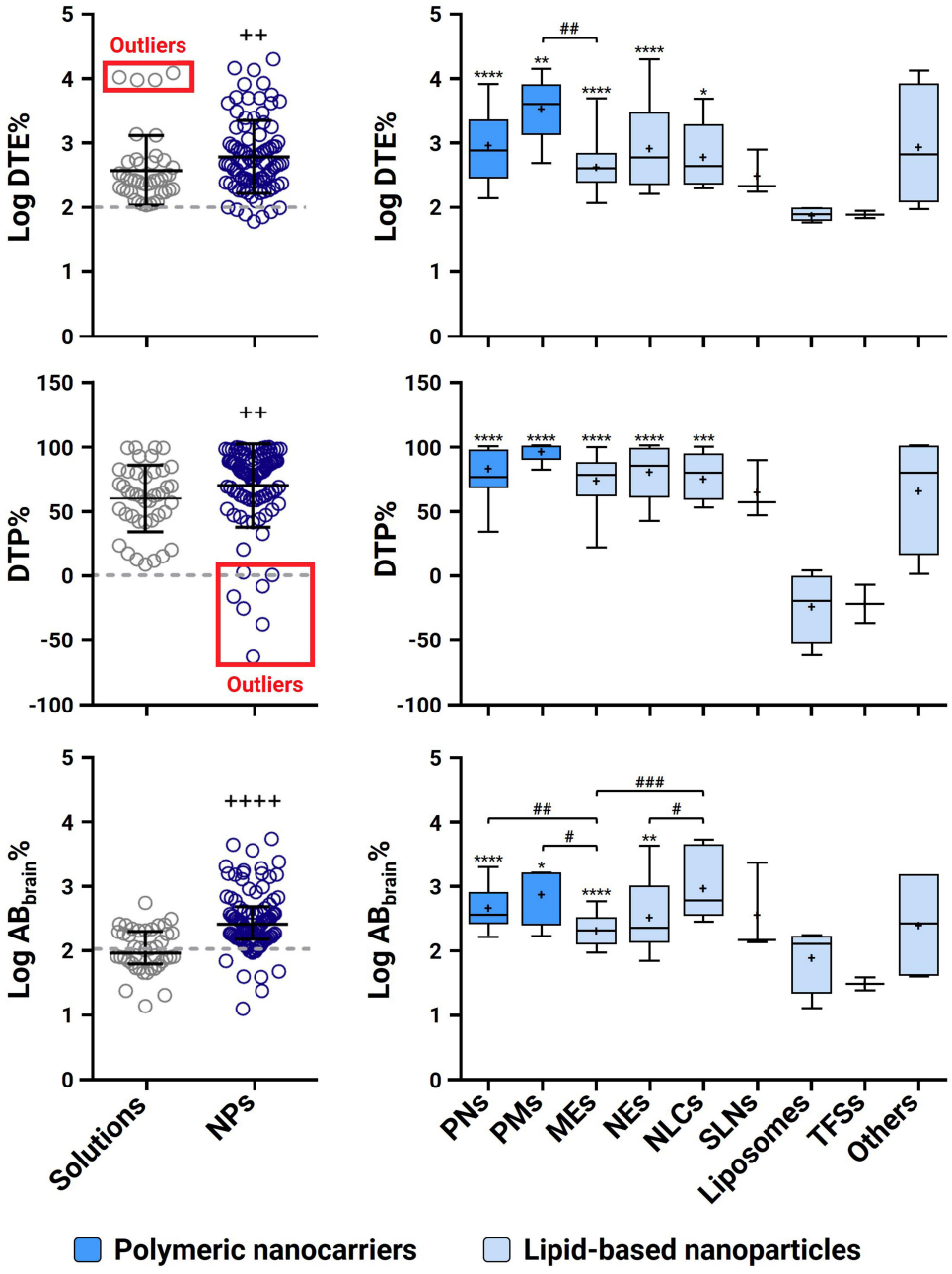

Figure 5 Comparison of overall drug delivered by nano systems and solutions. Box plots illustrating Log DTE %, Log DTP %, and Log ABbrain% for IN solutions and IN nanosystems showed the median, interquartile interval, and range, with the mean indicated by "+". Group mean comparisons were analyzed using one-way ANOVA with Tukey's post-test ($^{\#}p < 0.05$, $^{\#\#}p < 0.01$, and $^{\#\#\#}p < 0.001$). IN nanosystems and IN solutions were compared using the Mann–Whitney *U*-test (++p < 0.01, ++++p < 0.0001). Differences from reference "no-change" values were assessed by a one-sample *t*-test assuming normal distribution and a Wilcoxon signed-rank test when not assuming normal distribution (medians) (*p < 0.05, **p < 0.01, ***p < 0.001, ****p < 0.0001). Reprinted from *J Cont Rel*. Volume 270, Pires PC, Santos AO. Nanosystems in nose-to-brain drug delivery: a review of non-clinical brain targeting studies. J Cont Rel. 89–100. Copyright 2018, with permission from Elsevier.[47]

Abbreviations: AB_{brain}%, comparative brain bioavailability between IV and IN; IN, intranasal administration; IV, intravenous administration; ME, microemulsion; NE, nanoemulsion; NLC, nanostructured lipid carrier; NP, nanoparticle; PM, polymeric micelle; PN, polymeric nanoparticle; SLN, solid lipid nanoparticle; TFS, transfersome.

In-Situ Gel System

Recently, ISGs have emerged as a promising approach to address the challenges of nose-to-brain drug delivery through intranasal administration and to enhance drug uptake.[13] ISGs are clear or low-viscosity liquids before administration, but they convert into a viscous gel in response to nasal physiological conditions (pH, temperature, and ionic change). This prolongs the drug retention time in the nasal cavity, reduces the rapid elimination of the administered drug, and decreases the dose frequency. Table 4 summarizes the research on the use of ISGs for intranasal administration. Generally, the performance of ISGs is estimated using sol-gel transition temperature/time or titration tests.

Table 4 Temperature-, Ion-, and pH-Sensitive in-situ Gel (ISG) Researched for Nose-to-Brain Delivery

Drug (Indication)	ISG System	Optimized ISG Properties	Note	Ref.
Temperature-sensitive				
Rivastigmine tartrate (AD)	Pluronic F127 and Carbopol 934	• Tsg 27.2°C, Jss 258.62 μg/cm^2·h, and work of adhesion 11.1 J/m^2 • Shear-thinning behavior at storage and nasal temperatures	• The IN administration of ISG (IN) exhibited seven times higher DTE than the drug solution (IN), attributed to the mucoadhesive feature; DTP was 96.3%. • The ISG application implied an excellent drug delivery potential by the N2B route.	[98]
Almotriptan malate (migraine)	Pluronic F127, Pluronic F68, and carboxymethyl chitosan	• Tsg 34.10°C, GT 57.33 s, pH 6.31, drug content 95–96%, MS 476.678 Pa • Viscosity 49.82 and 764.30 mPa·s before and after gelation	• The ex-vivo histopathological images displayed any significant irritations on the sheep nasal mucosa. • The 60-day stability test of ISG demonstrated no considerable changes in Tsg, drug content, in-vitro dissolution profile, and viscosity.	[99]
Octreotide acetate (pituitary adenoma)	Poloxamer 407, HPMC K4M, and BAC	• Tsg 30.01°C, drug content 98.96%, and Jss 163.44 μg/cm^2·h • Viscosity 15.92 and 130.75 mPa·s before and after gelation	• The highest drug AUC in the brain and brain-to-blood ratio were achieved by the ISG (IN). • The ISG (IN) showed higher DTE and DTP than the free drug solution (IV).	[100]
Tranexamic acid (epistaxis)	Chitoclear FG and glycerophosphate	• Tsg 32°C, GT 5 min • Viscosity 0.15 and 269 Pa·s before and after gelation	• The ISG spray (IN) performances as the final dosage form were estimated: ovality ratio of 1.07; median droplet size of 99.7 μm, satisfying FDA and EMA criteria (30–120 μm). • A prolonged contact time on the nasal cavity was observed for the ISG by the nasal deposition profile.	[101]
Darunavir	Poloxamer 407, Carbopol 934P, PEG 400, PEG 6000, and methylparaben	• Tsg 30.5°C and Jss 49.83 μg/cm^2·h	• PEG 400 and PEG 6000 were used as solubilizers. • The ISG (IN) demonstrated about three times higher AUC than the drug solution (IV).	[102]
DB213 (HIV-associated neuronal disease)	Pluronic F127, Pluronic F68, and chitosan	• Tsg 31.6–32.2°C • Newtonian behavior at storage condition • Shear-thinning behavior at the nasal temperature	• The relative bioavailability of the ISG (IN) was described as 145% and 165% for mice and rats, respectively. • The drug concentration in the brain increased after post-administration for one hour.	[103]
Ion-sensitive				
Paroxetine (MDD)	DGG, HPMC E15 LV, and hydroxypropyl β-cyclodextrin	• GT 10–15 s, pH 6.2, drug content 99.29%, MS 499.363 Pa • Viscosity 49 mPa·s and 174 mPa·s before and after gelation	• The ISG (IN) induced faster onset of action than the drug suspension (PO), significantly reducing the average immobility time.	[104]
Vinpocetine (neuronal disease)	Carbopol 940, HPMC K4M, sodium alginate, and BAC	• pH within 4.53–4.64 • Viscosity ~800 and ~1800 mPa·s before and after gelation	• Although the optimized ion-sensitive ISG showed a lower AUC than the temperature-sensitive ISG, it presented a higher DTE (460%) and DTP (78.23%) than the counterpart (DTE of 390% and DTP of 74.30%), indicating a more brain-targeted delivery via the N2B route.	[105]

(*Continued*)

Table 4 (Continued).

Drug (Indication)	ISG System	Optimized ISG Properties	Note	Ref.
Rizatriptan benzoate (migraine)	DGG, HPMC E15 LV	• GT 12s, pH 6.2, drug content 99.51%, and MS 258.050 Pa	• The ex-vivo permeation rate of ISG at six hours was ~two times higher than that of the free drug solution. • There were no considerable changes in appearance, pH, GT, and drug content during the 60-day stability test under room and refrigerated conditions.	[106]
pH-sensitive				
Lamotrigine (epilepsy)	Medium molecular weight chitosan and sodium alginate	• GT 46s, pH 5.30, drug content 94.93%, and MS 19,000 Pa • Viscosity 341.66 and 2821 mPa s before and after gelation	• Increasing chitosan concentration led to a reduction of in-vitro drug permeation due to a strong viscous property. • The N2B route can obtain a higher drug concentration in the brain tissue.	[107]

Abbreviations: DTE, Drug-Targeting Efficiency; DTP, Drug Transport Percentage; GT, Gelation Time; in, Intranasal Administration; Jss, Steady-State Permeation Flux; MS, Mucoadhesive Strength; PO, Oral Administration; ST, Shear-Thinning (Pseudoplastic); Tsg, Sol-Gel Transition Temperature; indications; AD, Alzheimer's disease; MDD, major depressive disorder; Excipients; BAC, benzalkonium chloride; DDG, deacylated gellan gum; HPMC, hydroxypropyl methylcellulose; PEG, polyethylene glycol.

Mechanism of Sol-Gel Transition

ISGs can be classified into three types depending on the factors inducing the sol-gel transition within the nasal cavity: temperature-, ion-, and pH-sensitive ISGs.[13,108] Different gelling agents are employed depending on the type.

The sol-gel transition temperature of temperature-sensitive ISGs should be within 28–37°C to remain in a sol state during storage/administration and to change to a gel state in the body after administration.[13] Poloxamer® 407 (also known as Pluronic® F127) is a commonly used temperature-sensitive gelling agent that consists of hydrophilic end groups (PEO) and hydrophobic core groups (PPO).[98–100,102,103] With increasing temperature, the PPO block is dehydrated, which causes water expulsion from the micelle core, inducing gelation.

For ion-sensitive ISGs, gellan gum is commonly added as a gelling agent.[13,104,106] In gellan-gum-based systems, the sol-gel transition forms a double helical junction zone in response to interactions with cations, especially calcium ions, in the nasal fluid.[13,108,109] This conformational change further elicits a sol-gel transition by cationic complexation and hydrogen bond formation. Another ion-sensitive gelling agent, pectin, induces the sol-gel transition by the esterification-methoxylation of galacturonic acid.[13,110] The "egg box" model is the main sol-gel transition mechanism for pectin, in which dimerization induces calcium ions to crosslink two parallel galacturonic acid chains after being supported by hydrogen bonds and electrostatic forces.

Although pH-sensitive ISGs are less commonly investigated than other forms, they undergoes a conformational change and form a three-dimensional network using gelling agents, such as Carbopol® (poly acrylic acid).[13,107,108] The carboxylic acid groups in Carbopol® dissociate and uncoil when the pH is less than its pKa 5.5, forming a flexible and coiled structure.[13] In contrast, the alkaline environment of the human physiological nasal cavity facilitates the ionization of the carboxylic group, producing a negatively charged polymer backbone and finally forming a gel.

Drug Deposition of in-situ Gel Formulations in the Nasal Cavity

The ISG formulation can prolong the contact time of the drug in the nasal cavity due to sol-gel transition, depending on the nasal physiological conditions. After intranasal administration, confirming continuous drug release from a specific nasal cavity area is crucial.[111] However, several factors can disrupt drug deposition, including individual variations in nasal geometry, intranasal administration technique, and formulation characteristics (particle size and viscosity).[111,112] To address these limitations, researchers have studied how to predict drug deposition in the nasal cavity using in-vitro 3D models that mimic human nasal conditions or in-vivo models.[101,113–115] This section discusses drug deposition in the nasal cavity after intranasal administration of ISGs using a nasal device.

Li et al compared in-vivo nasal retention time between Cy7-loaded deacetylated gellan gum-based ISG and Cy7 solution using a mouse model (Figure 6A).[116] The ISG and control samples were administered intranasally to mice, and

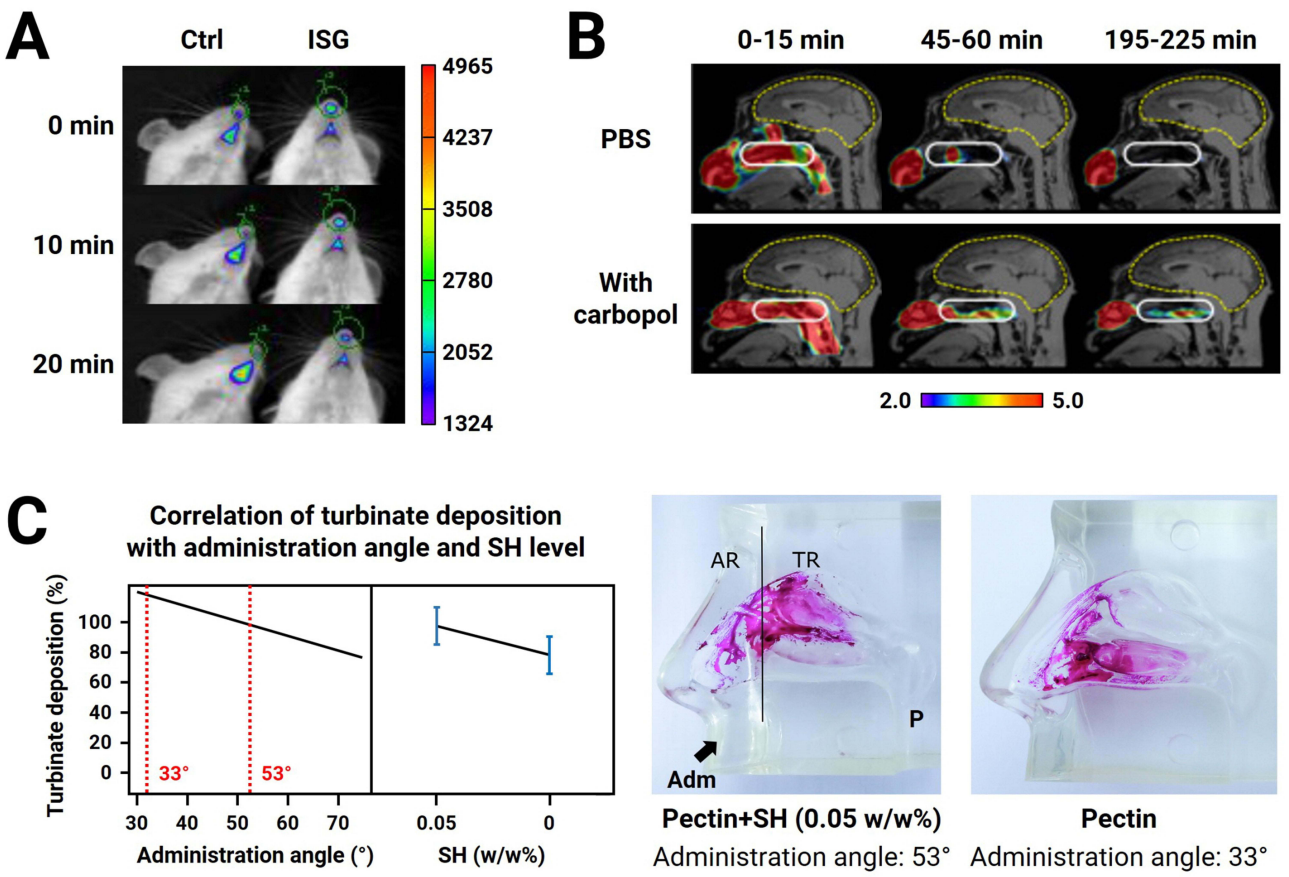

Figure 6 In-vivo and in-vitro drug deposition in the nasal cavity. (A) The Cy7 deposition in the nasal cavity after intranasal administration of solution (Ctrl) or gellan gum-based ISG. Reprinted from *Int J Pharm*. Volume 489 (1-2), Li X, Du L, Chen X, et al. Nasal delivery of analgesic ketorolac tromethamine thermo-and ion-sensitive in situ hydrogels. 252–260, Copyright 2015, with permission from Elsevier.[116] (B) PET images of rhesus monkey-head after intranasal administration of [^{18}F]-labeled vaccines mixed with PBS or ISG matrix. Reprinted from *Vaccine*. Volume 34(9), Saito S, Ainai A, Suzuki T, et al. The effect of mucoadhesive excipient on the nasal retention time of and the antibody responses induced by an intranasal influenza vaccine. 1201–1207, Copyright 2016, with permission from Elsevier.[117] (C) Effects of administration angle and excipient on the in-vitro 3D nasal deposition. Reprinted from *Int J Pharm*. Volume 563, Nižić L, Ugrina I, Špoljarić D, et al. Innovative sprayable in situ gelling fluticasone suspension: development and optimization of nasal deposition. 445–456. Copyright 2019, with permission from Elsevier.[113]
Abbreviations: Adm, administration; AR, anterior region; Ctrl, control; ISG, in-situ gel; P, pharynx; PBS, phosphate buffered saline; PET, positron emission tomography; SH, sodium hyaluronate; TR, turbinate region.

the dye distribution in the nasal cavity was profiled every five minutes. The ISG showed less dye entering from the oral cavity to the throat and higher dye deposition in the nasal cavity than the Cy7 solution, indicating a suitable drug absorption in the nasal cavity. In another animal model, Saito et al explored nasal cavity retention after intranasal administration of inactivated influenza vaccines conjugated with [^{18}F] using an in-vivo rhesus monkey model (Figure 6B).[117] The monkeys intranasally received the vaccine (250 μL in each nostril) through the nasal atomizer, and a positron emission tomography (PET) scanner scanned their heads. The vaccine prepared with the PBS medium was significantly less retained in the nasal cavity than the Carbopol-contained ISG, showing six-hour radioactivity remaining in the nasal cavity at 32.3% for the PBS-based group and 55.6% for the ISG group, respectively. Also, Cao et al formulated a gellan-gum-based ion-sensitive ISG containing scopolamine for treating motion sickness and profiled the in-vivo nasal deposition using 99mTc-DTPA.[111] The rabbits were rotated for 15 min after intranasal administration (100 μL) of the ISG and control solution, both containing 99mTc-DTPA, and scintigraphic images were captured. The authors found that a significant amount of the administered drug was distributed outside the nose as the experiment progressed and they concluded superior drug retention behavior for the ISG formulation than for the solution sample, suggesting the potential of reducing the drug dose when intranasal administration was applied.

Castile et al developed an in-vitro 3D nasal cast model to evaluate the in-situ gelling performance of PecSys®, a low-methoxy pectin-based ion-sensitive ISG technology patented in 2002[118], and compared the drug deposition of PecSys®

and a control solution (0.1 M phosphate buffer solution).[114] The test samples, which included fast green FCF dye, were sprayed using a 0.1 mL metered-dose nasal spray pump into the nostril of the 3D model. The ISG and control samples showed a similar level of dye deposition at the turbinate region immediately after spraying, but PecSys® showed significantly less dye movement towards the throat than the control after 120 s. The authors concluded that prolonged retention in the nasal cavity maximized drug absorption in the nasal mucosa. A similar result was observed in a study by Gholizadeh et al, who developed a chitosan-based temperature-sensitive ISG to treat epistaxis using tranexamic.[101] They evaluated drug deposition using an in-vitro 3D human nose model covered with Sar-Gel® paste, which changed color from white to purple in response to water molecules. They sprayed the ISG and drug solution (control) into the nostril using a VP3 spray device (Aptar, Crystal Lake, IL, USA) and visualized drug deposition for 20 min. Initially, the ISG showed a smaller initial deposition area than the control solution because of viscosity effects, and neither formulation passed through the throat, but backflowed slightly down to the throat. However, the ISG underwent gelation after 5 min, as the temperature exceeded the sol-gel transition temperature, and was retained in the nasal cavity, while the control solution moved toward the throat continuously.

Nižić and coworkers investigated the parameters influencing the drug deposition pattern after intranasal administration using an in-vitro 3D nasal model covered with Sar-Gel® paste.[113] They prepared a gellan-gum-based ion-sensitive ISG containing a fluticasone suspension and applied the spray pump system. Reducing the administration angle from the horizontal plane from 75° to 30° significantly enhanced drug deposition within the turbinate region. At an angle of 30°, the drugs were predominantly distributed in the lower part of the turbinate region. Furthermore, they found that the excipients used in the ISG affected the deposition pattern. The administration of ISG containing pectin and sodium hyaluronate (as a thickening agent) resulted in a higher distribution in the upper part of the turbinate region than the ISG containing pectin, despite the higher administration angle used for the ISG containing sodium hyaluronate (Figure 6C).

Conversely, Perkušić et al reported that drug deposition within the olfactory region was significantly influenced by administration parameters, rather than formulation parameters.[115] Enhanced drug deposition in the olfactory region was achieved with a higher administration angle, ranging from 45° to 75°, when intranasally delivering a chitosan-based temperature-sensitive ISG containing donepezil using the VP7 spray pump in an in-vitro 3D nasal model coated with Sar-Gel® paste. In addition, olfactory deposition was diminished by an increase in inspiratory flow rate, as breathing and airflow directed the formulation towards the turbinate region.

Nanoparticles with in-situ Gel Formulation

The combination of an ISG and the nanoparticle system alleviates the loss of the administered formulation by mucociliary clearance and facilitates nanoparticle uptake by the nasal membrane (Table 5).

Table 5 Formulation Design and Characterization of the Developed Optimal in-situ Gel (ISG) Loaded with Lipid-Based Nanoparticles (ISG-NP) for Nose-to-Brain Delivery. The Nanoparticle Properties Were Arranged Before and After Combining with ISG

Formulation Design			Characterization			Ref
Drug (Indication)	**Excipients**	**ISG matrix**	**Particle**	**Gel Stimuli**	**In-vivo Performance**	
Microemulsion						
Huperzine A (AD)	1,2-propanediol, castor oil, and Cremophor RH40	Pluronic F127, Pluronic F68, and chitosan	**Before** PS 21.26 nm, PDI 0.234, and ZP −28.3 mV **After** PS 20.53 nm, PDI 0.168, and ZP −21.9 mV	Tem. and pH	The ISG-NP (IN) showed a DTE of 100% and indicated that the drug could be absorbed into both the systemic circulation and N2B route.	[119]

(*Continued*)

Table 5 (Continued).

Formulation Design			Characterization			Ref
Drug (Indication)	**Excipients**	**ISG matrix**	**Particle**	**Gel Stimuli**	**In-vivo Performance**	
Nanoemulsion						
Disulfiram (GBM)	Ethyl oleate, Tween 80, Transcutol HP, and DSPE-PEG 2000	DGG	**Before** PS 90.51 nm and PDI 0.26 **After** PS 63.4 nm, PDI 0.168, and ZP −23.5 mV	Ion	The ISG-NP (IN) exhibited a superior anti-tumor effect and survival rate.	[120]
Rivastigmine (AD)	Miglyol 812, vitamin E, BAC, Tween 80, Phospholipon 90G, and glycerin	Poloxamer 407 and HPMC	**Before** PS 135.8 nm, PDI 0.1, ZP −20.9 mV, and EE 90.1% **After** PS 141.7 nm, PDI 0.4, ZP −4.1 mV, and EE 89.9%	Tem.	-	[121]
Clozapine (SCZ)	Oleic acid, Tween 80, propylene glycol	Poloxamer 407, BAC, sodium metabisulfite	**After** PS 17.7 nm, PDI 0.2, ZP −39.7 mV	Tem.	-	[122]
Amisulpride (SCZ)	Maisine CC, Labrasol, and Transcutol HP	Poloxamer 407 and DGG	**Before** PS 92.15 nm, PDI 0.46, ZP −18.22 mV, EE 99.01% **After** PS 106.11 nm, PDI 0.51, ZP −16.01 mV, and EE 98.93%	Tem.	The ISG-NP (IN) reduced locomotor activity and increased hind limb reaction time.	[123]
Dolutegravir (neuro-AIDS)	Dill oil, Tween 80, and Transcutol P	Poloxamer 407 and Carbopol 934P, and methylparaben	**Before** PS 106.36 nm, PDI 0.202, and ZP −18.22 mV	Tem.	The ISG-NP (IN) was absorbed into the N2B route quickly and released the drug sustainedly.	[124]
Liposome						
Opiorphin (Pain)	PC, CL, stearyl amine, and PEG-DSPE	Poloxamer 407 and Carbopol 934P	**Before** PS 141 nm, PDI 0.184, ZP −0.62 mV, and EE 59% **After** PS 143 nm, PDI 0.169, ZP −0.52 mV, and EE 58%	Tem.	-	[125]
Donepezil hydrochloride (AD)	HSPC and CL	DGG and xanthan gum	**Before** PS 103 nm and EE 93%	Ion	The biodistribution profile showed the highest drug deposition in the brain for the ISG-NP (IN).	[126]
Liposome; ethosome						
Apixaban (blood clot)	Lecithin, CL, and ethanol	Poloxamer 407, Poloxamer 188, and Carbopol 934	**Before** PS 145.1 nm, PDI 0.18, ZP −20 mV, and EE 67.11%	Tem.	The ISG-NP (IN) displayed the largest AUC resulting from avoiding the hepatic first-pass effect.	[127]

(*Continued*)

Table 5 (Continued).

Formulation Design			Characterization			Ref
Drug (Indication)	**Excipients**	**ISG matrix**	**Particle**	**Gel Stimuli**	**In-vivo Performance**	
Liposome; niosome						
Methotrexate (brain cancer)	CL and Span 60	Poloxamer 407, chitosan, and BGP	**Before** PS 259 nm, PDI 0.536, ZP −38.5 mV, and EE 91.39%	Tem.	The ISG-NP (IN) demonstrated the highest concentration ratio of brain/plasma.	[128]
Flibanserin (HSDD)	CL and Span 85	DGG	**Before** PS 46.35 nm and EE 92.48%	Ion	The ISG-NP (IN) showed higher AUC in the brain and plasma.	[129]
Buspirone hydrochloride (GAD)	CL and Span 60	Carbopol 974P and HPMC K15M	**Before** EE 70.57%	pH	The ISG-NP (IN) illustrated 6.85 times higher relative bioavailability than the drug solution (PO).	[130]
Liposome; transfersome						
Aripiprazole (SCZ)	PC and sodium deoxycholate	DGG	**Before** PS 72.12 nm, PDI 0.19, ZP −55.56 mV, and EE 97.06%	Ion	The ISG-NP (IN) could reduce locomotor activity and immobility time while increasing swimming and climbing times.	[131]
Rasagiline mesylate (PD)	PC and sodium deoxycholate	Pluronic 127, Pluronic F68, and pectin	**Before** PS 198.635 nm, PDI 0.45, ZP −33.45 mV, and EE 95.74%	Tem.	The ISG-NP (IN) showed a DTE of 304.53% and a DTP of 67.16%, confirming excellent brain delivery efficiency by the N2B route.	[132]
Resveratrol (AD)	Lecithin, Cremophor RH 40, and ethanol	Poloxamer 407 and Carbopol 934	**Before** PS 83.79 nm and EE 72.58%	Tem.	The ISG-NP (IN) presented 2.15 and 22.5 times higher Cmax and AUC than the drug suspension (PO).	[133]
Solid lipid nanoparticle (SLN)						
Piribedil (PD)	Palmitic acid and PVA	Methylcellulose and sodium chloride	**Before** PS 355.7 nm, PDI 0.125, ZP −18.34 mV, and EE 83% **After** PS 364.1 nm, PDI 0.126, and ZP −17.4 mV	Tem.	A similar Cmax between SLN (IN) and ISG-NP (IN) was observed, but the ISG-NP (IN) offered a higher AUC than the SLN (IN).	[134]
Curcumin (AD)	Compritol 888 ATO and Tween 80	Poloxamer 407, Poloxamer 188, and HPMC	**Before** PS 258.6 nm, PDI 0.354, ZP +19.3 mV, and EE 8% **After** PS 364.1 nm, PDI 0.126, and ZP −17.4 mV	Tem.	-	[135]
Almotriptan (migraine)	Precirol ATO 5, Phospholipon 90H, PVA, and Tween 80	Poloxamer 407 and carboxymethyl cellulose	**Before** PS 207.9 nm, PDI 0.41, ZP +19.3 mV, and EE 85% **After** PS 364.1 nm, PDI 0.126, and ZP −17.4 mV	Tem.	The ISG-NP (IN) enhanced a brain-targeting ability through the N2B route (DTP, 70%) and showed no significant nasal toxicity by biomarker study.	[136]

(*Continued*)

Table 5 (Continued).

Formulation Design			Characterization			Ref
Drug (Indication)	**Excipients**	**ISG matrix**	**Particle**	**Gel Stimuli**	**In-vivo Performance**	
Paeonol (neuronal disease)	GMS, lecithin, Poloxamer, and Tween 80	DGG, HPMC, glycerin, vitamin E, and chlorinated acetate	**Before** PS 166.79 nm, PDI 0.241, ZP −8.69 mV, and EE 88.72%	Ion	The ISG-NP (IN) convinced a prolongation of the nasal contact time by up to four hours and visualized the dye depositions in the olfactory bulb, cerebellum, and striatum.	[137]
Nanostructured lipid carrier (NLC)						
Resveratrol (AD)	Cetyl palmitate, Capmul MCM, Acrysol K150, Poloxamer 188, and Tween 80	DGG and xanthan gum	**Before** PS 132 nm, and EE 76%	Ion	The drug distribution of ISG-NP (IN) was the highest in the brain and lowest in the liver, among other organs, compared to the drug suspension (PO).	[138]
Teriflunomide (glioma)	Glyceryl di-behenate, glyceryl mono-linoleate, and Gelucire 4t/14	DGG and Carbopol 974P	**Before** PS 109.22 nm, PDI 0.52, ZP −24.92 mV, and EE 81.94% **After** PS 117.80 nm, PDI 0.56, ZP −21.86 mV, and EE 81.16%	Ion	The higher DTE value of 1500% in the ISG-NP (IN) than in other groups indicated significant drug delivery efficiency into the brain.	[139]
Rivastigmine (AD)	Precirol ATO 5, vitamin E, BAC, Tween 80, Phospholipon 90G, and glycerin	Poloxamer 407 and HPMC	**Before** PS 114.0 nm, PDI 0.2, ZP −30.6 mV, and EE 97.2% **After** PS 144.0 nm, PDI 0.5, ZP −3.6 mV, and EE 95.1%	Tem.	-	[121]
Lorazepam (status epilepticus)	GMS, oleic acid, and Pluronic F127	Chitosan and BGP	**Before** PS 71.7 nm, PDI 0.21, ZP −20.06 mV, and EE 81.80% **After** PS 165.46 nm and PDI 0.3	Tem.	The ISG-NP (IN) increased the lag time of epileptic seizure more than the other groups and alleviated the severity of symptoms in the trunk, hands, and feet.	[140]
Cinnarizine (migraine)	Cetyl palmitate, oleic acid, lecithin, and Pluronic F68	Pluronic F127, Pluronic F68, and chitosan	**Before** PS 108.9 nm, PDI 0.19, ZP −39.3 mV, and EE 97.7%	Tem.	The ISG-NP (IN) displayed about twice higher Cmax and AUC in the brain tissue than in the free drug solution (IN).	[141]
Flibanserin (HSDD)	Glyceryl behenate, almond oil, PC, and Gelucire 44/14	DGG	**Before** PS 114.63 nm, PDI 0.241, and ZP +8.4 mV	Ion	The ISG-NP (IN) facilitated the cellular uptake by lipophilic nanocarriers and offered higher AUC and Cmax than the ISG (IN).	[142]
Resveratrol (AD)	Cetyl palmitate, Capmul MCM, Acrysol K150, Poloxamer 188, and Tween 80	DGG and xanthan gum	**Before** PS 132 nm, PDI 0.209, ZP −23 mV, and EE 74.05%	Ion	The ISG-NP (IN) group gave the potential to improve cognitive functions in the scopolamine-induced AD model.	[143]
Clonazepam (epilepsy)	GMS, stearic acid, Compritol 888 ATO, oleic acid, and glycerol oleate	Pluronic F127 and sodium alginate	**Before** PS 210.2 nm, PDI 0.197, ZP −34.1 mV, and EE 65.7%	Tem.	The ISG-NP (IN) significantly delayed convulsion and death onset times by 1.5 and 5 times compared to the control group (no treatment).	[144]

(*Continued*)

Table 5 (Continued).

Formulation Design			Characterization			Ref
Drug (Indication)	**Excipients**	**ISG matrix**	**Particle**	**Gel Stimuli**	**In-vivo Performance**	
Donepezil (AD)	Glycerol di-stearate, Capmul MCM, Acrysol K150, Poloxamer 188, and Tween 80	DGG and xanthan gum	**Before** PS 112 nm, PDI 0.114, ZP −35 mV, and EE 79.25%	Ion	The ISG-NP (IN) presented a higher drug concentration in the brain comparing the marketed dosage product (PO).	[145]
Cannabidiol (CIPN)	Stearic acid, oleic acid, cetyl pyridinium chloride, and Span 20	Pluronic F127 and Pluronic F68	**Before** PS 177 nm, PDI 0.30, ZP +41 mV, and EE 99%	Tem.	The nociceptive threshold value was lower in the ISG-NP (IN) than in the control group (no treatment) in the paclitaxel-induced model.	[146]
Carbamazepine (epilepsy)	Precirol ATO 5, Capmul MCM, Tween 80, and Span 20	Poloxamer 407, Poloxamer 188, chitosan, and BAC	**Before** PS 132.8 nm, PDI 0.302, ZP −29.2 mV, and EE 89.73%	Tem.	The anticonvulsant activity was highest after treating the ISG-NP (IN).	[147]

Abbreviations: PS, Particle Size; PDI, Polydispersity Index; ZP, Zeta Potential; EE, Encapsulation Efficiency; DTE, Drug-Targeting Efficiency; in, Intranasal Administration; PO, Oral Administration; indications; AD, Alzheimer's disease; AIDS, acquired immunodeficiency syndrome; CIPN, chemotherapy-induced peripheral neuropathy; CVD, cardiovascular disease; GAD, generalised anxiety disorder; GBM, glioblastoma multiforme; HSDD, hypoactive sexual desire disorder; PD Parkinson's disease; SCZ, schizophrenia; Excipients; BAC, benzalkonium chloride; BGP, beta-glycerophosphate disodium salt hydrate; CL, cholesterol; DGG, deacylated gellan gum; DOTAP, 1.2-Dioleoyl-3-trimethylammonium propane; DSPC, distearoylphosphatidylcholine; DSPE, 1.2-distearoyl-sn-glycero-3-phosphoethanolamine; GMS, glycerol monostearate; HPMC, hydroxypropyl methylcellulose; HSPC, hydrogenated soy phosphatidylcholine; PC, phosphatidylcholine; PEG, polyethene glycol; The others; IN, intranasal; IV, intravenous; Tem., temperature.

Nanoemulsions

Gadhave et al designed a treatment strategy for schizophrenia by combining an amisulpride-loaded nanoemulsion (AMS-NE) with a temperature-sensitive ISG system (AMS-NE-ISG) based on Poloxamer® 407 and supported by gellan gum (Figure 7).[123] In-vitro drug release assessments using a dialysis membrane indicated that the rapid drug release observed with AMS-NE (100% at 4 h) could be attributed to the small nanoscale surface area of the nanoemulsion, resulting in easy permeation through the dialysis membranes. In contrast, AMS-NE-ISG displayed an improved sustained-release profile (~100% at 8 h). However, the AMS-NE-ISG showed a notably higher amount of ex-vivo drug permeation through the goat nasal mucosa than AMS-NE. This was due to the stronger mucoadhesiveness of AMS-NE-ISG, along with potential interactions between the polymers used for AMS-NE-ISG and the nasal membrane. In the context of an in-vivo pharmacokinetic study, the brain AUC results indicated that AMS-NE-ISG (intranasal) surpassed AMS-NE (intranasal) and AMS-NE (intravenous), signifying that the mucoadhesive and in-situ gelling polymers in AMS-NE-ISG contributed to its prolonged residence within the nasal cavity. Moreover, the higher DTP % of AMS-NE-ISG (275.09%) than AMS-NE (76.13%) confirmed that the combined formulation facilitated direct nose-to-brain delivery.

To treat Alzheimer's disease, Chen et al combined a Huperzine A-loaded microemulsion (Hup A-ME) with an ISG (Hup A-ME-ISG).[119] The authors employed a novel approach by incorporating Pluronic® polymers and chitosan as dual-sensitive in-situ gelling agents that are responsive to temperature and pH. The particle characteristics of Hup A-ME, with a particle size of ~20 nm, a PDI of ~0.2, and a zeta potential of −28 mV, exhibited minimal alterations after combining with the optimized gel matrix. Both formulations demonstrated a biphasic in-vitro drug release profile, with an initial burst release at 0.5 h followed by sustained release over 24 h. Similar to the findings from the study by Gadhave's group, the authors noted a slower drug release for Hup A-ME-ISG compared to Hup A-ME due to the presence of the Pluronic® polymer. In the context of pharmacokinetic investigation, the lipophilic nature of the microemulsion, the permeation-enhancing effect of chitosan, and the sol-gel transition performance collectively contributed to the ability of Hup A-ME-ISG (intranasal) to achieve higher absolute nasal bioavailability than both Hup A-ME (intranasal) and a Hup solution (intravenous).

Liposomes

Liposomes have been incorporated with ISGs as various derivatives, such as etosome,[127] niosome,[128–130] and transfersome,[131–133] which differ from intranasal administration alone. Rajput et al used a conventional liposome for a combination strategy with ISG by developing an ion-sensitive ISG containing donepezil-hydrochloride-loaded liposomes to treat Alzheimer's disease.[126] After

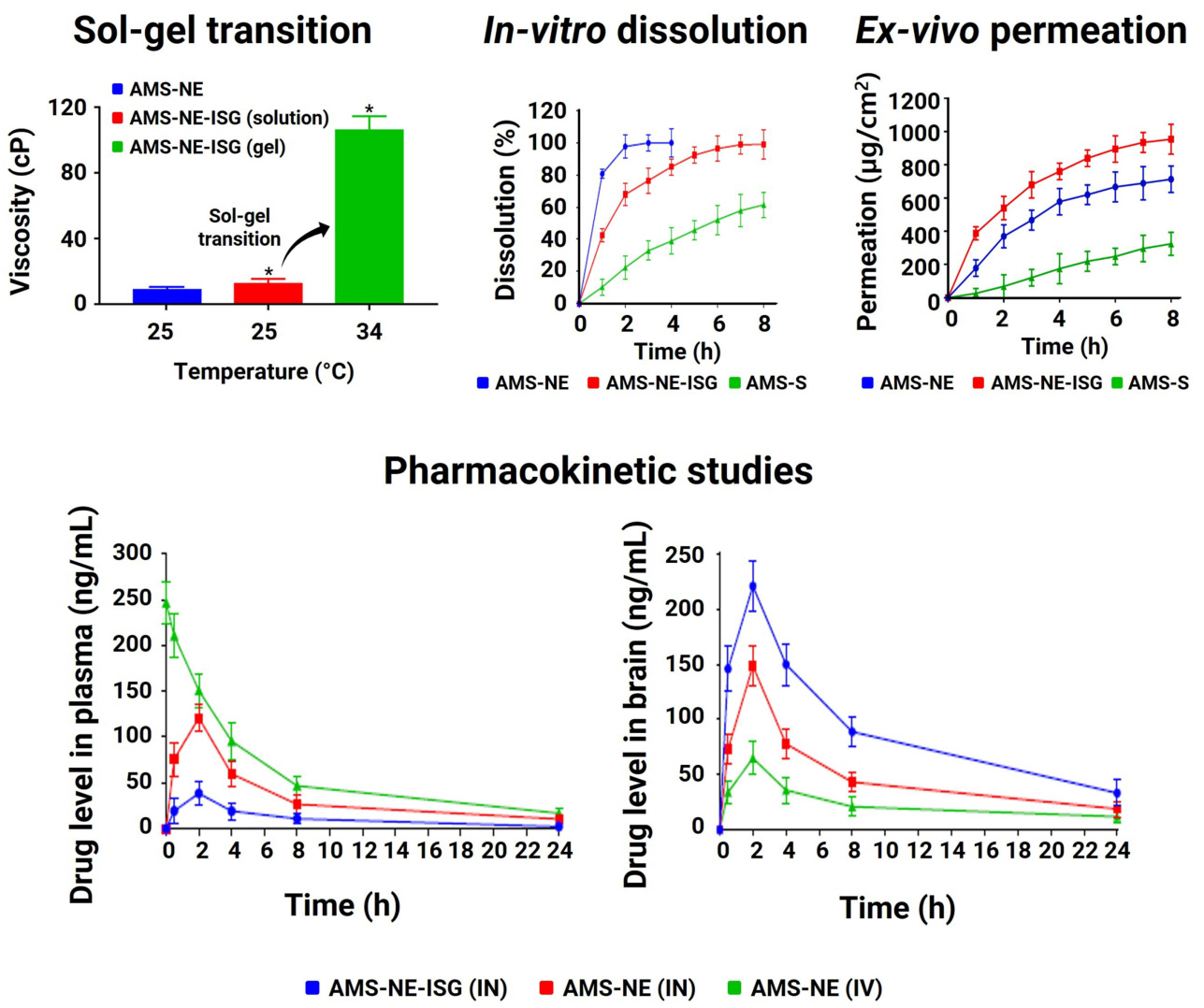

Figure 7 Sol-gel transition behavior, in-vitro dissolution profile using dialysis membrane, ex-vivo drug permeation, and pharmacokinetics studies of amisulpride-loaded nanoemulsion (AMS-NE) with a temperature-sensitive ISG system (AMS-NE-ISG) based on Poloxamer® 407 and supported by gellan gum. The significance level (*p < 0.05) indicates a statistically significant difference compared to the AMS-NE formulation. Reprinted from *Int J Pharm*. Volume 607, Gadhave D, Tupe S, Tagalpallewar A, Gorain B, Choudhury H, Kokare C. Nose-to-brain delivery of amisulpride-loaded lipid-based poloxamer-gellan gum nanoemulgel: in vitro and in vivo pharmacological studies. 121050. Copyright 2021, with permission from Elsevier.[123]

Abbreviations: AMS, amisulpride; NE, nanoemulsion; ISG, in-situ gel; IN, intranasal administration; IV, intravenous injection; S, suspension.

optimizing the combined formulation, an in vivo pharmacokinetic study was conducted to compare drug concentrations in the plasma and brain between oral administration of a marketed product and intranasal administration of the developed formulation. Intranasal administration of the optimized formulation (Cmax = ~ 600 ng/mL, tmax = 0.5 h) exhibited a plasma AUC 0.78 times the AUC of the orally administered product (Cmax = ~ 780 ng/mL, tmax = 2 h), whereas the brain AUC was significantly (3.28 times) higher for intranasal administration (Cmax = ~1240 ng/mL, tmax = 0.5 h) than oral administration (Cmax = ~ 380 ng/mL, tmax = 1 h). The authors mentioned that intranasal administration facilitated brain-targeted delivery (DTE % = 314.29%) owing to the nanoscale size and lipid nature of liposomes, which facilitated the transcellular transport of drug molecules via various endocytic pathways in sustentacular and neuronal cells within the olfactory membrane.

One of the liposome derivatives is ethosome, a flexible vesicular carrier containing a hydroalcoholic phospholipid with relatively higher alcohol concentrations.[148] It has demonstrated significantly greater penetration and release rates within the nasal membrane than conventional liposomes.[149,150] El-shenawy et al combined apixaban-loaded ethosome with an ISG to deliver the drug into the brain.[127] The authors optimized an apixaban-loaded ethosomal formulation comprising ethanol, soya

lecithin, and cholesterol. The encapsulation efficiency did not change with increasing concentrations of soy lecithin. Instead, it improved when the ethanol concentration was increased from 20% to 30% (v/v), owing to the enhanced solubility of apixaban in the inner polar core. However, a further increase in the ethanol concentration to 40% (v/v) reduced the encapsulation efficiency owing to membrane disruption and drug leakage. There was an inverse relationship between the vesicle size and ethanol concentration, which was attributed to the steric stabilization effect of ethanol, which induced a negative charge on the ethosome surfaces. Finally, they combined the optimal ethosome with a temperature-sensitive ISG and performed a pharmacokinetic study. Intranasal administration of the optimized formulation exhibited 5.5 times greater relative bioavailability than oral administration of the drug solution, which was attributed to the avoidance of the first-pass effect and enhanced drug permeation across the nasal mucosa.

Another derivative, the niosome, which is a bi-layered structure covered with nonionic surface-active agents, is characterized by reduced toxicity and enhanced compatibility. Recently, it has shown potential for application in brain-targeted delivery.[151] Ourani-Pourdashti et al studied the delivery of methotrexate into the brain using niosome-combined temperature-sensitive ISG via intranasal administration.[128] They determined the brain-targeting efficiency after intranasal administration of a methotrexate solution (free MTX), methotrexate-loaded ISG (MTX-ISG), methotrexate-loaded niosome (MTX-N), and MTX-N-loaded ISG (MTX-N-ISG). MTX-N-ISG surpassed the drug level in the brain compared to MTX-ISG and MTX-N, which showed a more significant proportion of the drug in the brain than free MTX. This was attributed to the advantages of the niosomal formulation, including mucoadhesive properties and sustained release behavior. Consequently, the brain/plasma ratio was the highest for MTX-N-ISG, indicating improved brain-targeting efficiency with few systemic adverse effects.

Transfersomes can also be used in nose-to-brain delivery systems. The transfersome, pioneered by Cevc and Blume, is the first generation of modified liposomes to have elastic and adaptable characteristics owing to edge activators, such as sodium cholate, bile salts, oleic acid, Span 80, and Tween 20.[150] Transfersomes can enhance penetration across significantly smaller pores than its particle size, thereby augmenting mucosal permeability within the paracellular tight junction.[150,152] El Shagea et al encapsulated rasagiline within transfersomes (RAS-T) and distributed them into a temperature-sensitive ISG (RAS-T-ISG; Pluronic® F-127 based and pectin supported) for the treatment of Parkinson's disease.[132] In the context of in-vitro release patterns, the burst drug release observed in RAS-T was significantly alleviated in RAS-T-ISG, which was attributable to the increased viscosity during the sol-gel transition. Following intranasal administration of RAS-T-ISG, notably elevated brain levels were evident compared to the intravenous administration of the free drug solution, and this was accompanied by lower drug concentrations in the plasma. The DTP % for RAS-T-ISG was 67.16%, underscoring the prevalence of direct nose-to-brain transport after intranasal administration. This may be attributed to the compact size of the transferosomes, the entanglement of the gelling agent with glycoprotein chains in the nasal mucosa, and the inclusion of a mucoadhesive polymer that diminished mucociliary clearance.

SLNs

Various SLN formulations have been modulated using ISG for nose-to-brain delivery. Uppuluri et al integrated piribedil-loaded SLN (RBD-SLN) with a methylcellulose-based temperature-sensitive ISG for treating Parkinson's disease (Figure 8).[134] The authors added sodium chloride to the ISG to induce the salting-out electrolyte effect and confirmed a decrease in the sol-gel transition temperature compared to the blank ISG solution devoid of sodium chloride. Interestingly, upon the integration of RBD-SLN into the ISG (RBD-SLN-ISG), a decrease in the sol-gel transition temperature and an increase in the gel strength of RBD-SLN-ISG were observed, possibly because of the higher concentration of suspended solid particles. Pharmacokinetic analysis was performed to profile the drug concentrations in both the plasma and brain following intranasal administration of the RBD suspension, RBD-SLN, and RBD-SLN-ISG. The in-vivo nasal residence time of RBD-SLN-ISG was 2.71 times greater than that of RBD-SLN. Although the initial drug concentrations in the brain were comparable between PBD-SLNs and PBD-SLN-ISGs, PBD-SLN-ISGs displayed higher drug concentrations than PBD-SLNs after 240 min. At the final time point (360 min), the drug levels declined below the quantification threshold for PBD-SLN, whereas PBD-SLN-ISG maintained concentrations above the limit of

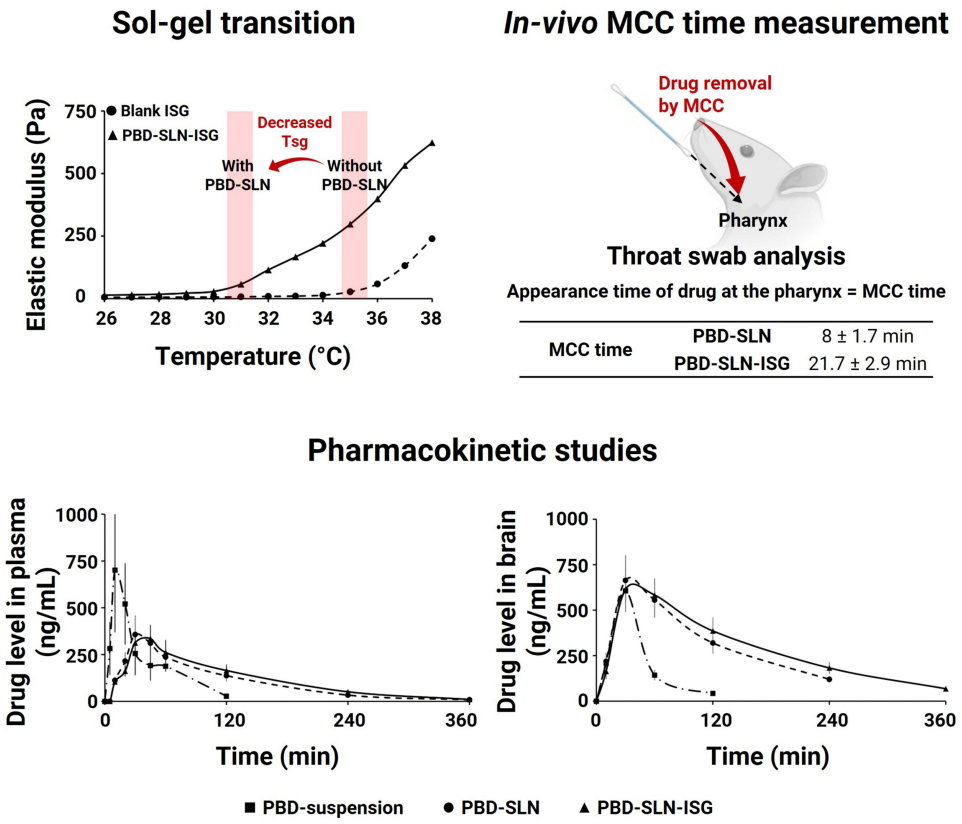

Figure 8 Sol-gel transition behavior, in-vivo comparative MCC time, and pharmacokinetic studies of piribedil-loaded SLN (RBD-SLN) with a methylcellulose-based temperature-sensitive ISG (PBD-SLN-ISG). Reprinted from *Int J Pharm*. Volume 606, Uppuluri CT, Ravi PR, Dalvi AV. Design, optimization and pharmacokinetic evaluation of piribedil loaded solid lipid nanoparticles dispersed in nasal in situ gelling system for effective management of Parkinson's disease. 120881. Copyright 2021, with permission from Elsevier.[134]

Abbreviations: Tsg, sol-gel transition temperature; PBD, piribedil; ISG, in-situ gel; SLN, solid lipid nanoparticle; MCC, mucociliary clearance.

quantification. This may be explained by the prolonged residence time of PBD-SLN-ISG, which led to a more sustained release profile.

Sun et al devised the combination strategy for the nose-to-brain delivery of the neuroprotective agent paeonol, which is challenged by poor water solubility and rapid metabolism, using an SLN-combined ion-sensitive ISG.[137] In the paeonol-loaded SLN (PAE-SLN), the disappearance of the characteristic peak of paeonol molecules in the XRD patterns signified the transformation of crystalline drug molecules to an amorphous or molecular state within the lipid matrix. The results of FTIR and DSC analyses corroborated this finding. PAE-SLN-integrated ISG (PAE-SLN-ISG) did not significantly alter the rheological behavior of blank ISG. For PAE-SLN-ISG, the low-viscosity Newtonian fluid properties of its liquid state suggested smooth administration and accurate deposition onto the olfactory mucosa. In contrast, the gel state exhibited non-Newtonian pseudoplastic characteristics that facilitated the erosion of the administered gel and drug release in response to the motion of the nasal cilia. PAE-SLN-ISG displayed two distinct in-vitro drug release patterns: PAE-SLN release from the optimal formulation and PAE release from the SLN carrier. Moreover, the authors conducted an in-vivo study of nasal residence using the fluorescent probe cyanine 7 NHS ester (Cy7). Intranasal administration of Cy7-SLN-ISG resulted in a fluorescence response within the brain regions, which accumulated in the brain until the duration of the experiment.

NLCs

NLCs have been studied more extensively than other lipid-based formulations. Gadhave et al performed nose-to-brain delivery of teriflunomide using an NLC with an ion-sensitive ISG formulation for glioma treatment.[139] The formulation contained gellan gum as the gelling agent and Carbopol® 974P as the mucoadhesive agent. From XRD and DSC

analyses, the authors established that the drug molecules were encapsulated in an amorphous state within the final formulation, ISG-containing teriflunomide-loaded NLCs (TER-NLC-ISG). Ex-vivo nasal permeation assessments encompassing parameters such as steady-state flux, permeability coefficient, and the amount of drug permeated, indicated that TER-NLC-ISGs outperformed TER-loaded NLCs (TER-NLCs). This may be attributed to the mucoadhesive agent, which prolonged the nasal residence time, and the surfactant and gellan gum, which facilitated the opening of tight junctions. Upon intranasal administration, the notably higher DTE % of TER-NLC-ISGs (1500%) compared to TER-NLC (DTE % = 92%) highlighted a superior propensity for nose-to-brain delivery. The in-vivo biodistribution analysis corroborated these findings, revealing higher drug concentrations in the brain following intranasal administration of TER-NLC-ISGs than following intravenous administration of TER-NLCs.

To deliver rivastigmine to treat Alzheimer's disease via the nose-to-brain route, Cunha et al developed different lipid-based nanoparticles, nanoemulsions (RIV-NE), and NLCs (RIV-NLC).[121] They integrated them into temperature-sensitive ISGs, referred to as RIV-NE-ISG and RIV-NLC-ISG, respectively. Their study included a comprehensive comparison of various parameters between RIV-NE-ISG and RIV-NLC-ISG, encompassing drug deposition profiles within the nasal cavity. While no significant differences were observed in terms of particle size, PDI, zeta potential, encapsulation efficiency, or loading capacity between RIV-NE-ISG and RIV-NLC-ISG, RIV-NLC-ISG exhibited higher viscosity and more sustained drug release than RIV-NE-ISG. This was attributed to the lipid composition, as NLCs possess a solid matrix composed of lipids and oil, whereas nanoemulsions only contain lipids. However, RIV-NLC-ISG and RIV-NE-ISG exhibited comparable mucoadhesive profiles. Drug deposition was assessed using the Alberta Idealized Throat model by administering the formulated samples via a nasal spray. The ISG demonstrated increased drug deposition in the turbinate and olfactory regions compared to nanoparticles alone, suggesting the potential for nose-to-brain delivery.

Challenges in Intranasal Administration for Drug Delivery

Toxicology

As mentioned previously, nasal mucociliary clearance is the defense mechanism preventing the entrance of harmful substances, and ciliated cells are related to this clearance process. However, the nasal physiological conditions, such as pH and osmolarity, can be altered after intranasal administration, potentially inducing nasal irritation.[32,153] The mucociliary clearance function relies heavily on the mucosal pH.[153] Thus, intranasal formulations must comply with acceptable pH to mitigate the risk of nasal irritation. Osmolality, another critical factor related to mucociliary beats, also influences nasal toxicity.[32,153] The inhibition of mucociliary clearance by several specific moieties can induce congestion, dryness, irritation, and sneezing.[153] While in-vitro models can assess these physiological parameters, achieving precise reproducibility in in-vivo settings for evaluating side effects remains a formidable challenge.

Material Challenge

Understanding the safety of intranasal nanoparticle systems is crucial, and it is essential to examine the safety of excipients and adjuvants beyond the drug itself.[13,153] Excipients incorporated in intranasal formulations can affect retention time in the nasal cavity and protect drugs from enzymatic degradation. However, benzalkonium chloride, which has inhibitory effects on ciliary beats, can lead to dose and time-dependent toxicity. Similarly, penetration enhancers may facilitate drug permeation across the nasal epithelium but also have disruptive properties, resulting in undesired effects. Although many molecules are natural irritants to nasal physiology, they typically do not cause permanent damage. Nonetheless, it underscores the necessity to evaluate the toxicological challenges associated with intranasal nanoparticle systems, where understanding the intricate dynamics of formulation components becomes integral to ensuring both efficacy and safety.

Differences Between in-vivo and in-vitro Models

In the case of in-situ gel, the evaluations of sol-gel transition performance are preferentially conducted by in-vitro experiments measuring changes in viscosity or rheological properties. Once the in-vitro sol-gel transition is established,

the subsequent validation of gelation behavior and nasal deposition progresses to in-vivo models utilizing living animals. Nonetheless, challenges arise from the anatomical distinctions between humans and other animals,[154] hindering a precise extrapolation of the effectiveness when administering intranasal formulations for humans. Therefore, recent efforts have seen the development of an innovative in-vitro 3D model reproducing the nasal cavity of an actual human. These advancements have led to research publications on reconciling anatomical disparities between humans and animals. It aims to bridge the translational gap in assessing the performance of intranasal formulations, offering a more human-relevant perspective in preclinical studies.

Targeting Properties

As mentioned in the section "Factors affecting intranasal drug delivery", the residence time of the intranasal formulation in the nasal cavity is short because of mucociliary clearance, ultimately showing low brain-targeting efficiency. In other words, brain-targeting efficiency can be improved by increasing the time the drug is released into the nasal cavity and when the drug is absorbed in the nasal epithelium; therefore, mucoadhesive nanoparticles and gel systems have emerged.

For the mucoadhesive nanoparticles, the mucoadhesive polymers capable of penetrating the mucus layer can enhance the potential adhesive interactions at the nasal mucosa.[155] The low molecular mucoadhesive polymers devoid of cross-linkages facilitate the penetration into the mucus network, impeding the interpenetration process —however, the polymers with short chains and limited crosslinking exhibit low cohesion. Consequently, the adhesive bond typically does not fail at the mucus-polymer interface. Instead, it tends to break within the polymeric network. Therefore, the selected polymers for intranasal formulations should also display adequate cohesion stabilizing interactions between polymer chains; it can be acquired by utilizing gel system.

Disease Selectivity

In various studies, it has been observed that when drugs follow the olfactory nerve pathway after intranasal administration, they distribute more prominently in the forebrain than the hindbrain.[63,156] This observation holds significance in the context of diseases that frequently manifest in the forebrain, such as glioblastoma, suggesting the potential effectiveness of intranasal administration for therapeutic intervention. Conversely, drugs enter the brain through the pons and medulla for the trigeminal nerve pathway,[7] raising expectations for efficacy in medulloblastoma treatment.[157] However, it is worth noting that utilizing specific nose-to-brain delivery pathways for exclusive drug transport to the brain necessitates further extensive research in this area.

Towards the Clinical Translation of Intranasal Administration Technologies

Nose-to-brain-targeted intranasal administration products continue to undergo development, with several noteworthy examples of products that have successfully achieved clinical realization. These products provide tangible evidence for the potential and versatility of intranasal drug delivery for brain-targeted therapies. Table 6 provides a reference point detailing approved drugs that have been intranasally administered for various medical applications. Among these pioneering products is an esketamine nasal spray (Spravato; Johnson & Johnson, New Brunswick, NJ, USA), which has gained approval for the treatment of depression. Additionally, sumatriptan nasal spray is a viable option for alleviating migraines via intranasal delivery. Another example is Narcan nasal spray, which is designed to counter opioid overdoses by swiftly administering naloxone via the nasal route. These examples highlight the versatility of intranasal administration in addressing a wide range of medical needs. The detailed information for the clinical trials of applying intranasal administration to nose-to-brain delivery is summarised in Table 7.

Furthermore, intranasal drug delivery research is witnessing robust activity in the utilization of nanotechnology. Although intranasal products incorporating nanotechnology are not currently at the forefront of research activities, the integration of QbD principles is being harnessed to increase the potential of translating nanotechnology-based intranasal products into clinical practice. This strategic implementation aims to enhance the predictability, quality, and efficiency of these innovative intranasal pharmaceuticals.[14,158] QbD is a systematic approach applied during the manufacturing of formulations to ensure consistent and high-quality outcomes. It involves several interconnected steps that help optimize

Table 6 Representative FDA-Approved Intranasal Product in the Market for Nose-to-Brain Delivery

Active Ingredient(s)	Indication	DOSAGE FORM	Brand Name (Company)
Butorphanol tartrate	Opioid narcotic pain reliever	Metered spray	Butorphanol tartrate nasal spray (Rising Pharma Holdings, Inc.)
Diazepam	Stereotypic episodes	Spray	Valtoco® (Neurelis Inc.)
Dihydroergotamine mesylate	Migraine	Metered spray	Migranal® (Bausch Health US LLC) Trudhesa® (Impel Pharmaceuticals Inc.)
Esketamine HCl	Major depressive disorder	Spray	Spravato® (Janssen Pharmaceuticals Inc.)
Naloxone HCl	Opioid overdose	Metered spray	Narcan® (Emergent Operations Ireland ltd.)
Sumatriptan	Migraine	Spray	Imitrex® (GlaxoSmithKline) Tosymra® (Tonix Medicines Inc.)
Sumatriptan succinate	Migraine	Powder spray	Onzetra® Xsail® (Currax Pharmaceuticals LLC)

Abbreviations: HCl, hydrochloride.

Table 7 Clinical Trials for the Intranasal Administration for Nose-to-Brain Delivery, Which are Under Recruiting, Enrolling, or Completed Status, to Treat Alzheimer's Disease, Parkinson's Disease, Migraine, Schizophrenia, Major Depressive Disorder, and Stroke

Drug (product)	Con.	Study title	Phase (Start Date)	Status (Enrollment)	NTC Number
AL-108	SCZ	A Multicenter Study of NAP (AL-108) in Schizophrenia	Phase 2 (July, 2007)	Completed (63)	NCT00505765
Autologous M2 macrophages	MD	Intranasal Inhalations of Bioactive Factors Produced by M2 Macrophages in Patients With Organic Brain Syndrome	Phase 1, 2 (March, 2016)	Completed (30)	NCT02957123
B244	M	Study to Determine Safety and Efficacy of B244 in Subjects With Episodic Migraine	Phase 2 (March, 2018)	Completed (313)	NCT03488563
Bone marrow stem cell	AD	Alzheimer's Autism and Cognitive Impairment Stem Cell Treatment Study (ACIST)	Not applicable (October, 2018)	Enrolling (100)	NCT03724136
Bone marrow stem cell	PD	Neurologic Stem Cell Treatment Study (NEST)	Not applicable (June, 2016)	Recruiting (500)	NCT02795052
Cromoglicate	SCZ	Cromoglicate Adjunctive Therapy for Outpatients With Schizophrenia (CATOS)	Phase 1, 2 (April, 2019)	Recruiting (160)	NCT03794076
Diazepam (NRL-1)	E	Repeat-Dose Pharmacokinetics Study of NRL-1 in Epilepsy Subjects	Phase 1 (June, 2016)	Completed (57)	NCT02724423
Diazepam (NRL-1)	E	Repeat Dose Safety Study of NRL-1 in Epilepsy Subjects	Phase 3 (April, 2016)	Completed (175)	NCT02721069
Dihydroergotamine	M	A Phase I Study to Study the PK and Safety of Single Doses of STS101, DHE Injection and Nasal Spray in Healthy Subjects	Phase 1 (September, 2018)	Completed (46)	NCT03874832
Dihydroergotamine Mesylate with POD	M	Bioavailability of DHE Administered by 1123 POD Device, IV Injection, and Migranal Nasal Spray in Healthy Adults	Phase 1 (October, 2017)	Completed (36)	NCT03401346
Dihydroergotamine Mesylate with POD	M	Safety and Tolerability of POD-DHE (INP104) in Migraine (STOP 301)	Phase 3 (July, 2018)	Completed (360)	NCT03557333
Esketamine	MDD	A Long-term Comparison of Esketamine Nasal Spray Versus Quetiapine Extended Release, Both in Combination With a Selective Serotonin Reuptake Inhibitor/ Serotonin-Norepinephrine Reuptake Inhibitor, in Participants With Treatment Resistant Major Depressive Disorder (ESCAPE-TRD)	Phase 3 (August, 2020)	Completed (676)	NCT04338321
Esketamine	MDD	54135419SUI3001: A Study to Evaluate the Efficacy and Safety of Intranasal Esketamine in Addition to Comprehensive Standard of Care for the Rapid Reduction of the Symptoms of Major Depressive Disorder, Including Suicidal Ideation, in Adult Participants Assessed to be at Imminent Risk for Suicide (Aspire I)	Phase 3 (December, 2018)	Completed (226)	NCT03039192

(*Continued*)

Table 7 (Continued).

Drug (product)	Con.	Study title	Phase (Start Date)	Status (Enrollment)	NTC Number
Esketamine	MDD	54135419SUI3002: A Study to Evaluate the Efficacy and Safety of Intranasal Esketamine in Addition to Comprehensive Standard of Care for the Rapid Reduction of the Symptoms of Major Depressive Disorder, Including Suicidal Ideation, in Adult Participants Assessed to be at Imminent Risk for Suicide (Aspire II)	Phase 3 (June, 2017)	Completed (230)	NCT03097133
Esketamine	MDD	A Long-term Safety Study of Esketamine Nasal Spray in Treatment-resistant Depression (SUSTAIN-3)	Phase 3 (June, 2016)	Completed (1148)	NCT02782104
Esketamine	MDD	A Double-blind Study to Assess the Efficacy and Safety of Intranasal Esketamine for the Rapid Reduction of the Symptoms of Major Depressive Disorder, Including Suicidal Ideation, in Participants Who Are Assessed to be at Imminent Risk for Suicide	Phase 2 (May, 2014)	Completed (68)	NCT02133001
Esketamine and midazolam	MDD	Study to Evaluate the Efficacy and Safety of 3 Fixed Doses of Intranasal Esketamine in Addition to Comprehensive Standard of Care for the Rapid Reduction of the Symptoms of Major Depressive Disorder, Including Suicidal Ideation, in Pediatric Participants Assessed to be at Imminent Risk for Suicide	Phase 2 (October, 2017)	Completed (147)	NCT03185819
Glutathione	PD	Phase IIb Study of Intranasal Glutathione in Parkinson's Disease ((in)GSH)	Phase 2 (April, 2015)	Completed (45)	NCT02424708
Glutathione	PD	CNS Uptake of Intranasal Glutathione	Phase 1 (December, 2014)	Completed (15)	NCT02324426
Glutathione	PD	Intranasal Glutathione in Parkinson's Disease	Phase 1 (July, 2012)	Completed (34)	NCT01398748
Insulin	SCZ	Effects of Intranasal Insulin on Neuroimaging Markers and Cognition in Patients With Psychotic Disorders	Phase 2 (October, 2019)	Recruiting (90)	NCT03943537
Insulin	Stroke	Intranasal Insulin and Post-stroke Cognition: A Pilot Study	Phase 2 (April, 2016)	Completed (20)	NCT02810392
Insulin	AD	Study of Nasal Insulin to Fight Forgetfulness - Short-Acting Insulin Aspart (SNIFF-Quick)	Phase 1 (March, 2015)	Completed (24)	NCT02462161
Insulin	PD	Treatment of Parkinson Disease and Multiple System Atrophy Using Intranasal Insulin	Phase 2 (February, 2014)	Completed (15)	NCT02064166
Insulin	MDD	Effect of Intranasal Insulin on Depressive Symptoms in Major Depressive Disorder	Phase 3 (June, 2013)	Completed (35)	NCT00570050
Insulin	SCZ	Intranasal Insulin Treatment in Patients With Schizophrenia	Phase 4 (December, 2007)	Completed (45)	NCT00575666
Insulin	AD	Memory and Insulin in Early Alzheimer's Disease (MAIN)	Phase 1, 2 (October, 2007)	Completed (31)	NCT00581867
Insulin	SCZ	Effect of Single Dose Intranasal Insulin On Cognitive Function	Phase 4 (October, 2006)	Completed (30)	NCT00646581
Insulin	AD	SNIFF 120: Study of Nasal Insulin to Fight Forgetfulness (120 Days) (SNIFF 120)	Phase 2 (June, 2006)	Completed (173)	NCT00438568
Insulin (Humulin® R U-100)	MDD	Brain Insulin Resistance in Mood Disorders	Phase 1, 2 (October, 2021)	Recruiting (150)	NCT03915613
Insulin (Humulin® R U-100)	AD	The Study of Nasal Insulin in the Fight Against Forgetfulness (SNIFF)	Phase 2, 3 (January, 2014)	Completed (240)	NCT01767909
Insulin (Humulin® R U-100) and emagliflozin	AD	SNIFF - Combo INI+EMPA Trial	Phase 2 (October, 2021)	Recruiting (60)	NCT05081219
Insulin (Levemir®)	AD	Study of Nasal Insulin to Fight Forgetfulness - Long-acting Insulin Detemir - 120 Days (SL120) (SL120)	Phase 2 (November, 2011)	Completed (37)	NCT01595646

(*Continued*)

Table 7 (Continued).

Drug (product)	Con.	Study title	Phase (Start Date)	Status (Enrollment)	NTC Number
Insulin (Levemir®)	AD	Study of Nasal Insulin to Fight Forgetfulness - Long-acting Insulin Detemir - 21 Days (SNIFF-LONG 21)	Phase 2 (March, 2011)	Completed (60)	NCT01547169
Insulin (Novolin® R)	PD	Intranasal Insulin in Parkinson's Disease (INI-PD)	Phase 2 (February, 2020)	Recruiting (30)	NCT04251585
Insulin glulisine	AD	Safety and Effectiveness Study of Intranasal Insulin Glulisine on Cognitive and Memory in Mild-Mod AD Patients.	Phase 2 (September, 2011)	Completed (12)	NCT01436045
Insulin with glutathione	PD	Intranasal Insulin and Glutathione as an Add-On Therapy in Parkinson's Disease (NOSE-PD)	Phase 2 (February, 2022)	Recruiting (56)	NCT05266417
Ketamine	MDD	A Study of SLS-002 (Intranasal Racemic Ketamine) in Adults With Major Depressive Disorder at Imminent Risk of Suicide	Phase 2 (December, 2020)	Recruiting (236)	NCT04669665
Ketamine	MDD	A Study to Evaluate the Effects of a Single-Dose and Repeat-Administration of Intranasal Esketamine on On-Road Driving in Participants With Major Depressive Disorder (DriveSaFe2)	Phase 1 (October, 2016)	Completed (27)	NCT02919579
Ketamine	MDD	Intra-nasal vs Intra-venous Ketamine Administration	Phase 4 (April, 2016)	Completed (45)	NCT02644629
Ketorolac	M	Intranasal Ketorolac Versus Intravenous Ketorolac for Treatment of Migraine Headaches in Children	Phase 3 (June, 2015)	Completed (59)	NCT02358681
Ketorolac tromethamine	M	Efficacy and Safety of Intranasal Ketorolac for the Acute Treatment of Migraine	Phase 2 (July, 2007)	Completed (173)	NCT00483717
Levodopa	PD	Therapeutic Potential for Intranasal Levodopa in Parkinson's Disease -Off Reversal (THOR201)	Phase 2 (May, 2018)	Completed (32)	NCT03541356
Lidocaine	M	A Pilot Study of Intranasal Lidocaine in Acute Management of Pediatric Migraine	Phase 1 (July, 2019)	Completed (30)	NCT03806595
Lidocaine	M	Intranasal Lidocaine to Treat Pediatric Migraine in the Emergency Department	Phase 3 (October, 2018)	Unknown; recruiting (50)	NCT03576820
Lidocaine, bupivacaine, and ropivacain	M	Sphenopalatine Ganglion Blocks RCT (SPGblock)	Phase 4 (February, 2019)	Completed (10)	NCT03666663
Nerve growth factors	Ischemic stroke	Effects of Intranasal Nerve Growth Factor for Acute Ischemic Stroke	Phase 4 (January, 2016)	Completed (106)	NCT03686163
Nicotine	PD	Pilot Trial of Transnasal Nicotine in Parkinson Disease	Phase 2 (March, 2019)	Completed (6)	NCT03865121
Olanzapine with POD device	SCZ and BD	Safety and Tolerability of INP105 (Olanzapine by I231 POD® Device) Nasal Spray in Healthy Volunteers - SNAP 101 (SNAP101)	Phase 1 (August, 2018)	Completed (38)	NCT03624322
Oxytocin	SCZ	Target Engagement and Response to Oxytocin	Phase 4 (January, 2018)	Completed (120)	NCT03245437
Oxytocin	MDD	Emotional Processing and Oxytocin Mechanisms in Premenstrual Dysphoric Disorder: A Pilot Study	Phase 2 (July, 2015)	Completed (10)	NCT02508103
Oxytocin	MDD	Therapy With an Oxytocin Adjunct for Major Depression (TOAD2015)	Phase 2 (February, 2015)	Completed (24)	NCT02405715
Oxytocin	M	TI-001 (Intranasal Oxytocin) for Treatment of High Frequency Episodic Migraine and Chronic Migraine	Phase 2 (May, 2013)	Completed (240)	NCT01839149
Oxytocin	SCZ	Effects of Intranasal Oxytocin on Satiety Signaling in People With Schizophrenia	Phase 4 (June, 2012)	Completed (24)	NCT01614093

(*Continued*)

Table 7 (Continued).

Drug (product)	Con.	Study title	Phase (Start Date)	Status (Enrollment)	NTC Number
Oxytocin	SCZ	Oxytocin Treatment of Social Cognitive and Functional Deficits in Schizophrenia (OTS-12WK)	Phase 2 (July, 2011)	Completed (68)	NCT01394471
Oxytocin	SCZ	Adult Study Oxytocin - Behavioral (ASO-Behavioral)	Early Phase 1 (October, 2010)	Completed (324)	NCT02567032
Sumatriptan	M	Bioavailability Study to Compare OPTINOSE SUMATRIPTAN With IMITREX® in Healthy Subjects	Phase 1 (January, 2012)	Completed (20)	NCT01507610
Sumatriptan (Onzetra® Xsail)	M	Study to Assess the Safety and Efficacy of ONZETRA® Xsail® for the Acute Treatment of Episodic Migraine With or Without Aura in Adolescents	Phase 3 (November, 2017)	Completed (159)	NCT03338920
TNX-1900	M	A Study to Evaluate the Efficacy and Safety of TNX-1900 in Patients With Chronic Migraine (PREVENTION)	Phase 2 (December, 2022)	Recruiting (300)	NCT05679908
Zavegepant	M	Randomized Trial in Adult Participants With Acute Migraines	Phase 3 (October, 2020)	Completed (1978)	NCT04571060
Zavegepant	M	Long-term Safety Study of BHV-3500 (Zavegepant*) for the Acute Treatment of Migraine	Phase 2, 3 (June, 2020)	Completed (974)	NCT04408794
Zolmitriptan	M	A Four-way Crossover Study of 3 Formulations of M207 With Intranasal Zolmitriptan in Healthy Volunteers	Phase 1 (May, 2019)	Completed (24)	NCT03978403
Zolmitriptan (Zomig®)	M	A Study of M207 With Intranasal Zolmitriptan in Healthy Volunteers	Phase 1 (November, 2018)	Completed (24)	NCT03708744
Zolmitriptan (Zomig®)	M	Efficacy & Safety Of Zomig Nasal Spray For Acute Migraine Treatment In Subjects 6 To 11 Years, With OLE	Phase 3 (November, 2017)	Completed (374)	NCT03275922

Abbreviations: AD, Alzheimer's disease; BD, bipolar disorder; E, epilepsy; M, Migraine; MDD, major depressive disorder; PD, Parkinson's disease; POD, precision olfactory delivery; SCZ, schizophrenia; MD, mental disorder.

the formulation process and end-product quality. QbD is used in the manufacture of lipid-based nanoparticles and ISG formulations for nose-to-brain delivery.[159–162]

1) Quality Target Product Profile (QTPP): The process begins by defining the desired attributes of the drug delivery system, including parameters such as drug release kinetics, stability (for lipid-based nanoparticles), gel viscosity, drug release kinetics, and nasal retention time (for ISGs). The QTPP forms the foundation for identifying the critical quality attributes (CQAs) that require control to achieve the desired product objectives.
2) Critical Quality Attribute (CQA): CQAs that significantly influence the quality and effectiveness of a drug delivery system are identified. For lipid-based nanoparticles, CQAs can include attributes such as particle size, size distribution, surface charge, and drug-loading efficiency. For ISGs, CQAs may involve factors such as gelation time, temperature, and rheological properties.
3) Critical Material Attribute (CMA): The CMAs determine the material properties of the components used in both formulations that may impact the final product. In lipid-based nanoparticles, CMAs may include the attributes of the lipids, surfactants, and drugs. For ISGs, the CMAs may include the characteristics of polymers, solvents, and drug molecules.
4) Critical Process Parameter (CPP): The crucial variables within the manufacturing process that significantly affect the quality of both formulations are identified. This may involve parameters such as the homogenization speed and temperature during formulation (for lipid-based nanoparticles), the mixing speed, and pH adjustment during gelation (for ISGs).
5) Design of Experiments (DoE): DoE techniques are employed to systematically vary the CMAs and CPPs for both formulations to understand their effects on CQAs. This experimentation phase aids in establishing correlations and optimizing the formulation processes.

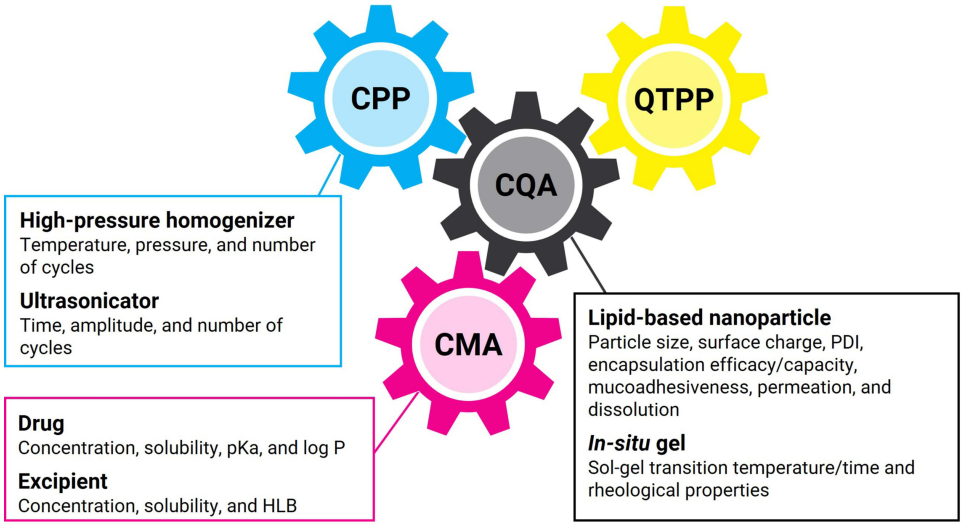

Figure 9 Illustration of the quality by design (QbD) framework for the development of lipid-based nanoparticle and in-situ gel systems. QbD has the potential to facilitate the development of effective nose-to-brain delivery systems. The components of QbD, such as critical process parameters (CPP), critical material attributes (CMA), critical quality attributes (CQA), and the quality target product profile (QTPP), interact and influence each other, providing feedback within the design space. The representative parameters of CPP, CMA, and CQA are listed.
Abbreviations: PDI, polydispersity index; HLB, hydrophilic-lipophilic balance.

6) Design Space: A range of acceptable values for the CMAs and CPPs within which the desired CQAs are consistently achieved are defined. This design space provides manufacturing flexibility, while maintaining product quality.
7) Risk assessment and mitigation: Potential risks that may affect the quality of both formulations, such as drug instability and inadequate nasal absorption, are identified and assessed. Strategies to manage or mitigate these risks are then implemented.
8) Continuous Monitoring and Improvement: After establishing the formulations within their respective design spaces, monitoring systems are implemented to ensure that the manufacturing processes remain within the defined parameters. Any deviations are then investigated and addressed promptly.

By applying QbD to the development of both ISG- and lipid-based nanoparticle formulations for intranasal drug delivery, we can ensure that the final products consistently meet quality standards, align with their desired attributes, and effectively deliver drugs through the intranasal route. The detailed factors related to QbD are shown in Figure 9.

Conclusion

In this paper, various aspects of nose-to-brain drug delivery were explored. The primary focus was on two methods: utilizing small lipid-based particles to transport drugs, and employing adaptable gels for controlled drug release within the nasal cavity. These approaches have the potential to revolutionize drug delivery from the nose to the brain. This paper provides a thorough review of the multifaceted nature of this specialized delivery method. Emphasis was been placed on its benefits, such as rapid drug absorption and the circumvention of specific digestive processes. Additionally, challenges stemming from the intricacies of the nasal structure and formulation complexities were addressed. Real-world experiences gleaned from clinical trials were shared to underscore the considerable promise of these methods in enhancing drug efficacy, while ensuring patient friendliness. However, persistent challenges remain. Therefore, it is imperative to ensure substance stability, precise drug dosing, and long-term safety. Given the unique nasal structures of individuals and the potential adverse effects of intranasally delivered drugs, rigorous experimentation and comprehensive risk assessments are essential prerequisites for their broad-scale adoption.

In summary, we elucidated the potential utility of lipid-based particles and adaptable gels for the advancement of nose-to-brain drug delivery via intranasal administration. Despite these significant strides, sustained research, development, and experimentation are vital to fully harness the advantages of these techniques and pave the way for their effective integration into clinical practice.

Acknowledgments

This work was supported by the National Research Foundation of Korea (NRF), which is funded by the Korean government (MSIT) [grant nos. 2021R1A2C2008519, 2022R1C1C2002949, and 2022R1A5A6000760].

Disclosure

The authors declare that they have no conflicts of interest in this work.

References

1. Kaushik A, Jayant RD, Bhardwaj V, Nair M. Personalized nanomedicine for CNS diseases. *Drug Discovery Today*. 2018;23(5):1007–1015. doi:10.1016/j.drudis.2017.11.010
2. Nichols E, Szoeke CE, Vollset SE, et al. Global, regional, and national burden of Alzheimer's disease and other dementias, 1990–2016: a systematic analysis for the global burden of disease study 2016. *Lancet Neurol*. 2019;18(1):88–106. doi:10.1016/S1474-4422(18)30403-4
3. Dorsey ER, Elbaz A, Nichols E, et al. Global, regional, and national burden of Parkinson's disease, 1990–2016: a systematic analysis for the global burden of disease study 2016. *Lancet Neurol*. 2018;17(11):939–953. doi:10.1016/S1474-4422(18)30295-3
4. Charlson FJ, Ferrari AJ, Santomauro DF, et al. Global epidemiology and burden of schizophrenia: findings from the global burden of disease study 2016. *Schizophrenia Bulletin*. 2018;44(6):1195–1203. doi:10.1093/schbul/sby058
5. Wallin MT, Culpepper WJ, Nichols E, et al. Global, regional, and national burden of multiple sclerosis 1990–2016: a systematic analysis for the global burden of disease study 2016. *Lancet Neurol*. 2019;18(3):269–285. doi:10.1016/S1474-4422(18)30443-5
6. Patel AP, Fisher JL, Nichols E, et al. Global, regional, and national burden of brain and other CNS cancer, 1990–2016: a systematic analysis for the global burden of disease Study 2016. *Lancet Neurol*. 2019;18(4):376–393. doi:10.1016/S1474-4422(18)30468-X
7. Agrawal M, Saraf S, Saraf S, et al. Nose-to-brain drug delivery: an update on clinical challenges and progress towards approval of anti-Alzheimer drugs. *J Cont Rel*. 2018;281:139–177. doi:10.1016/j.jconrel.2018.05.011
8. Liu H-J, Xu P. Strategies to overcome/penetrate the BBB for systemic nanoparticle delivery to the brain/brain tumor. *Advan Drug Del Rev*. 2022;191:114619. doi:10.1016/j.addr.2022.114619
9. Kapoor M, Cloyd JC, Siegel RA. A review of intranasal formulations for the treatment of seizure emergencies. *Journal of Controlled Release*. 2016;237:147–159. doi:10.1016/j.jconrel.2016.07.001
10. Wong KH, Riaz MK, Xie Y, et al. Review of current strategies for delivering Alzheimer's disease drugs across the blood-brain barrier. *Internat J Mol Sci*. 2019;20(2):381. doi:10.3390/ijms20020381
11. Reddy S, Tatiparti K, Sau S, Iyer AK. Recent advances in nano delivery systems for blood-brain barrier (BBB) penetration and targeting of brain tumors. *Drug Discovery Today*. 2021;26(8):1944–1952. doi:10.1016/j.drudis.2021.04.008
12. Formica ML, Real DA, Picchio ML, Catlin E, Donnelly RF, Paredes AJ. On a highway to the brain: a review on nose-to-brain drug delivery using nanoparticles. *Applied Materials Today*. 2022;29:101631. doi:10.1016/j.apmt.2022.101631
13. Agrawal M, Saraf S, Saraf S, et al. Stimuli-responsive in situ gelling system for nose-to-brain drug delivery. *J Cont Rel*. 2020;327:235–265. doi:10.1016/j.jconrel.2020.07.044
14. Akel H, Ismail R, Csoka I. Progress and perspectives of brain-targeting lipid-based nanosystems via the nasal route in Alzheimer's disease. *Europ J Pharmaceut Biopharmac*. 2020;148:38–53. doi:10.1016/j.ejpb.2019.12.014
15. Sabir F, Ismail R, Csoka I. Nose-to-brain delivery of antiglioblastoma drugs embedded into lipid nanocarrier systems: status quo and outlook. *Drug Discovery Today*. 2020;25(1):185–194. doi:10.1016/j.drudis.2019.10.005
16. Feng Y, He H, Li F, Lu Y, Qi J, Wu W. An update on the role of nanovehicles in nose-to-brain drug delivery. *Drug Discovery Today*. 2018;23(5):1079–1088. doi:10.1016/j.drudis.2018.01.005
17. Khan AR, Liu M, Khan MW, Zhai G. Progress in brain targeting drug delivery system by nasal route. *J Cont Rel*. 2017;268:364–389. doi:10.1016/j.jconrel.2017.09.001
18. Pardridge WM. Treatment of Alzheimer's disease and blood-brain barrier drug delivery. *Pharmaceuticals*. 2020;13(11):394. doi:10.3390/ph13110394
19. Delhaas E, Huygen F. Complications associated with intrathecal drug delivery systems. *BJA Educ*. 2020;20(2):51–57. doi:10.1016/j.bjae.2019.11.002
20. Terstappen GC, Meyer AH, Bell RD, Zhang W. Strategies for delivering therapeutics across the blood-brain barrier. *Nat Rev Drug Discov*. 2021;20(5):362–383. doi:10.1038/s41573-021-00139-y
21. Costa CP, Moreira JN, Lobo JMS, Silva AC. Intranasal delivery of nanostructured lipid carriers, solid lipid nanoparticles and nanoemulsions: a current overview of in vivo studies. *Acta Pharmac Sinica B*. 2021;11(4):925–940. doi:10.1016/j.apsb.2021.02.012
22. Dkhar LK, Bartley J, White D, Seyfoddin A. Intranasal drug delivery devices and interventions associated with post-operative endoscopic sinus surgery. *Pharmac Develop Technol*. 2018;23(3):282–294. doi:10.1080/10837450.2017.1389956
23. Goel H, Kalra V, Verma SK, Dubey SK, Tiwary AK. Convolutions in the rendition of nose to brain therapeutics from bench to bedside: feats & fallacies. *J Control Rel*. 2022;341:782–811. doi:10.1016/j.jconrel.2021.12.009
24. Dogan R, Senturk E, Ozturan O, Yildirim YS, Tugrul S, Hafiz AM. Conchal contractility after inferior turbinate hypertrophy treatment: a prospective, randomized clinical trial. *Am J Otolaryngol*. 2017;38(6):678–682.

25. Jeong S-H, Jang J-H, Lee Y-B. Drug delivery to the brain via the nasal route of administration: exploration of key targets and major consideration factors. *J Pharmac Invest*. 2023;53(1):119–152. doi:10.1007/s40005-022-00589-5
26. Crowe TP, Hsu WH. Evaluation of recent intranasal drug delivery systems to the central nervous system. *Pharmaceutics*. 2022;14(3):629. doi:10.3390/pharmaceutics14030629
27. Vincent AJ, West AK, Chuah MI. Morphological and functional plasticity of olfactory ensheathing cells. *J Neurocytol*. 2005;34(1–2):65–80. doi:10.1007/s11068-005-5048-6
28. Inoue D, Furubayashi T, Tanaka A, Sakane T, Sugano K. Effect of cerebrospinal fluid circulation on nose-to-brain direct delivery and distribution of caffeine in rats. *Molec Pharmaceut*. 2020;17(11):4067–4076. doi:10.1021/acs.molpharmaceut.0c00495
29. Fukuda M, Kanazawa T, Iioka S, et al. Quantitative analysis of inulin distribution in the brain focused on nose-to-brain route via olfactory epithelium by reverse esophageal cannulation. *Journal of Controlled Release*. 2021;332:493–501. doi:10.1016/j.jconrel.2021.02.024
30. Tashima T. Shortcut approaches to substance delivery into the brain based on intranasal administration using nanodelivery strategies for insulin. *Molecules*. 2020;25(21):5188. doi:10.3390/molecules25215188
31. Crowe TP, Greenlee MHW, Kanthasamy AG, Hsu WH. Mechanism of intranasal drug delivery directly to the brain. *Life Sci*. 2018;195:44–52. doi:10.1016/j.lfs.2017.12.025
32. Costa C, Moreira J, Amaral M, Lobo JS, Silva AC. Nose-to-brain delivery of lipid-based nanosystems for epileptic seizures and anxiety crisis. *J Cont Rel*. 2019;295:187–200. doi:10.1016/j.jconrel.2018.12.049
33. Cone RA. Barrier properties of mucus. *Advan Drug Deliv Rev*. 2009;61(2):75–85. doi:10.1016/j.addr.2008.09.008
34. Froehlich E, Roblegg E. Mucus as barrier for drug delivery by nanoparticles. *J Nanosci Nanotechnol*. 2014;14(1):126–136. doi:10.1166/jnn.2014.9015
35. Wu L, Shan W, Zhang Z, Huang Y. Engineering nanomaterials to overcome the mucosal barrier by modulating surface properties. *Advan Drug Deliv Rev*. 2018;124:150–163. doi:10.1016/j.addr.2017.10.001
36. Patel AA, Patel RJ, Patel SR. Nanomedicine for intranasal delivery to improve brain uptake. *Curr Drug Deliv*. 2018;15(4):461–469. doi:10.2174/1567201814666171013150534
37. Arora P, Sharma S, Garg S. Permeability issues in nasal drug delivery. *Drug Discovery Today*. 2002;7(18):967–975. doi:10.1016/S1359-6446(02)02452-2
38. Kaur P, Garg T, Rath G, Goyal AK. In situ nasal gel drug delivery: a novel approach for brain targeting through the mucosal membrane. *Artif Cells Nanomed Biotechnol*. 2016;44(4):1167–1176. doi:10.3109/21691401.2015.1012260
39. Jain H, Prabhakar B, Shende P. Modulation of olfactory area for effective transportation of actives in CNS disorders. *J Drug Deliv Sci Technol*. 2022;68:103091. doi:10.1016/j.jddst.2021.103091
40. Warnken ZN, Smyth HD, Watts AB, Weitman S, Kuhn JG, Williams RO. Formulation and device design to increase nose to brain drug delivery. *J Drug Deliv Sci Technol*. 2016;35:213–222. doi:10.1016/j.jddst.2016.05.003
41. Xu J, Tao J, Wang J. Design and application in delivery system of intranasal antidepressants. *Front Bioeng Biotechnol*. 2020;8:626882. doi:10.3389/fbioe.2020.626882
42. Sánchez-Dengra B, González-Álvarez I, Bermejo M, González-Álvarez M. Access to the CNS: strategies to overcome the BBB. *Internat J Pharmac*. 2023;636:122759. doi:10.1016/j.ijpharm.2023.122759
43. Pandit R, Chen L, Götz J. The blood-brain barrier: physiology and strategies for drug delivery. *Advan Drug Deliv Rev*. 2020;165–166:1–14. doi:10.1016/j.addr.2019.11.009
44. Mitusova K, Peltek OO, Karpov TE, Muslimov AR, Zyuzin MV, Timin AS. Overcoming the blood–brain barrier for the therapy of malignant brain tumor: current status and prospects of drug delivery approaches. *J Nanobiotechnol*. 2022;20(1):412.
45. Correia A, Monteiro A, Silva R, Moreira J, Lobo JS, Silva A. Lipid nanoparticles strategies to modify pharmacokinetics of central nervous system targeting drugs: crossing or circumventing the blood-brain barrier (BBB) to manage neurological disorders. *Advan Drug Deliv Rev*. 2022;189:114485. doi:10.1016/j.addr.2022.114485
46. Nguyen TT, Nguyen TTD, Tran N, Van Vo G. Lipid-based nanocarriers via nose-to-brain pathway for central nervous system disorders. *Neuroch Res*. 2022;2022:1–22.
47. Pires PC, Santos AO. Nanosystems in nose-to-brain drug delivery: a review of non-clinical brain targeting studies. *J Cont Rel*. 2018;270:89–100. doi:10.1016/j.jconrel.2017.11.047
48. Shah D, Guo Y, Ban I, Shao J. Intranasal delivery of insulin by self-emulsified nanoemulsion system: in vitro and in vivo studies. *Internat J Pharmac*. 2022;616:121565. doi:10.1016/j.ijpharm.2022.121565
49. Jiang Y, Liu C, Zhai W, Zhuang N, Han T, Ding Z. The optimization design of lactoferrin loaded Hup A nanoemulsion for targeted drug transport via intranasal route. *Internat J Nanomed*. 2019;Volume 14:9217–9234. doi:10.2147/IJN.S214657
50. Kaur A, Nigam K, Bhatnagar I, et al. Treatment of Alzheimer's disease using donepezil nanoemulsion: an intranasal approach. *Drug Deliv Translat Res*. 2020;10(6):1862–1875. doi:10.1007/s13346-020-00754-z
51. Mallick A, Gupta A, Hussain A, et al. Intranasal delivery of gabapentin loaded optimized nanoemulsion for augmented permeation. *J Drug Deliv Sci Technol*. 2020;56:101606. doi:10.1016/j.jddst.2020.101606
52. Arora A, Kumar S, Ali J, Baboota S. Intranasal delivery of tetrabenazine nanoemulsion via olfactory region for better treatment of hyperkinetic movement associated with Huntington's disease: pharmacokinetic and brain delivery study. *Chem Phys Lip*. 2020;230:104917. doi:10.1016/j.chemphyslip.2020.104917
53. Ashhar MU, Kumar S, Ali J, Baboota S. CCRD based development of bromocriptine and glutathione nanoemulsion tailored ultrasonically for the combined anti-Parkinson effect. *Chem Phys Lip*. 2021;235:105035. doi:10.1016/j.chemphyslip.2020.105035
54. Gaba B, Khan T, Haider MF, et al. Vitamin E loaded naringenin nanoemulsion via intranasal delivery for the management of oxidative stress in a 6-OHDA Parkinson's disease model. *BioMed Res Internat*. 2019;2019:1–20. doi:10.1155/2019/2382563
55. Diedrich C, Zittlau IC, Machado CS, et al. Mucoadhesive nanoemulsion enhances brain bioavailability of luteolin after intranasal administration and induces apoptosis to SH-SY5Y neuroblastoma cells. *Internat J Pharmac*. 2022;626:122142. doi:10.1016/j.ijpharm.2022.122142
56. Fachel FNS, Medeiros-Neves B, Dal Prá M, et al. Box-Behnken design optimization of mucoadhesive chitosan-coated nanoemulsions for rosmarinic acid nasal delivery-in vitro studies. *Carbohy Pol*. 2018;199:572–582. doi:10.1016/j.carbpol.2018.07.054

57. Ahmad N, Ahmad R, Amir M, et al. Ischemic brain treated with 6-gingerol loaded mucoadhesive nanoemulsion via intranasal delivery and their comparative pharmacokinetic effect in brain. *J Drug Deliv Sci Technol*. 2021;61:102130. doi:10.1016/j.jddst.2020.102130
58. Patel RJ, Parikh RH. Intranasal delivery of topiramate nanoemulsion: pharmacodynamic, pharmacokinetic and brain uptake studies. *Internat J Pharmac*. 2020;585:119486. doi:10.1016/j.ijpharm.2020.119486
59. Kaur A, Nigam K, Srivastava S, Tyagi A, Dang S. Memantine nanoemulsion: a new approach to treat Alzheimer's disease. *J Microencapsul*. 2020;37(5):355–365. doi:10.1080/02652048.2020.1756971
60. Iqbal R, Ahmed S, Jain GK, Vohora D. Design and development of letrozole nanoemulsion: a comparative evaluation of brain targeted nanoemulsion with free letrozole against status epilepticus and neurodegeneration in mice. *Internat J Pharmac*. 2019;565:20–32. doi:10.1016/j.ijpharm.2019.04.076
61. Shen X, Cui Z, Wei Y, et al. Exploring the potential to enhance drug distribution in the brain subregion via intranasal delivery of nanoemulsion in combination with borneol as a guider. *As J Pharmac Sci*. 2023;18(6):100778. doi:10.1016/j.ajps.2023.100778
62. Nogueira C, Lemos-Senna E, da Silva Vieira E, et al. β-caryophyllene cationic nanoemulsion for intranasal delivery and treatment of epilepsy: development and in vivo evaluation of anticonvulsant activity. *J Nanopart Res*. 2023;25(1):19. doi:10.1007/s11051-023-05668-8
63. Kurano T, Kanazawa T, Ooba A, et al. Nose-to-brain/spinal cord delivery kinetics of liposomes with different surface properties. *J Cont Rel*. 2022;344:225–234. doi:10.1016/j.jconrel.2022.03.017
64. Barros C, Aranha N, Severino P, et al. Quality by design approach for the development of liposome carrying ghrelin for intranasal administration. *Pharmaceutics*. 2021;13(5):686. doi:10.3390/pharmaceutics13050686
65. Pashirova TN, Zueva IV, Petrov KA, et al. Mixed cationic liposomes for brain delivery of drugs by the intranasal route: the acetylcholinesterase reactivator 2-PAM as encapsulated drug model. *Coll Surf B*. 2018;171:358–367. doi:10.1016/j.colsurfb.2018.07.049
66. Katona G, Sabir F, Sipos B, et al. Development of lomustine and n-propyl gallate co-encapsulated liposomes for targeting glioblastoma multiforme via intranasal administration. *Pharmaceutics*. 2022;14(3):631. doi:10.3390/pharmaceutics14030631
67. Sabir F, Katona G, Pallagi E, et al. Quality-by-design-based development of n-propyl-gallate-loaded hyaluronic-acid-coated liposomes for intranasal administration. *Molecules*. 2021;26(5):1429. doi:10.3390/molecules26051429
68. Saka R, Chella N, Khan W. Development of imatinib mesylate-loaded liposomes for nose to brain delivery: in vitro and in vivo evaluation. *AAPS Pharm Sci Tech*. 2021;22(5):192. doi:10.1208/s12249-021-02072-0
69. Singh V, Krishan P, Shri R. Amelioration of ischaemia reperfusion-induced cerebral injury in mice by liposomes containing Allium cepa fraction administered intranasally. *Artif Cells Nanomed Biotechnol*. 2018;46(sup3):982–992. doi:10.1080/21691401.2018.1523181
70. Yuwanda A, Surini S, Harahap Y, Jufri M. Study of valproic acid liposomes for delivery into the brain through an intranasal route. *Heliyon*. 2022;8(3):e09030. doi:10.1016/j.heliyon.2022.e09030
71. Taha MS, Kutlehria S, D'Souza A, Bleier BS, Amiji MM. Topical administration of verapamil in poly (ethylene glycol)-modified liposomes for enhanced sinonasal tissue residence in chronic rhinosinusitis: ex vivo and in vivo evaluations. *Molecu Pharmaceut*. 2023;20(3):1729–1736. doi:10.1021/acs.molpharmaceut.2c00943
72. Trapani A, De Giglio E, Cometa S, et al. Dopamine-loaded lipid based nanocarriers for intranasal administration of the neurotransmitter: a comparative study. *Europ J Pharmac Biopharm*. 2021;167:189–200. doi:10.1016/j.ejpb.2021.07.015
73. Wang L, Zhao X, Du J, Liu M, Feng J, Hu K. Improved brain delivery of pueraria flavones via intranasal administration of borneol-modified solid lipid nanoparticles. *Nanomedicine*. 2019;14(16):2105–2119. doi:10.2217/nnm-2018-0417
74. Hasan N, Imran M, Kesharwani P, et al. Intranasal delivery of naloxone-loaded solid lipid nanoparticles as a promising simple and non-invasive approach for the management of opioid overdose. *Internat J Pharmac*. 2021;599:120428. doi:10.1016/j.ijpharm.2021.120428
75. Said DE, Amer EI, Sheta E, Makled S, Arafa FM, Diab HE. Nano-encapsulated antioxidant: retinoic acid as a natural mucosal adjuvant for intranasal immunization against chronic experimental toxoplasmosis. *Trop Med Infect Dis*. 2023;8(2):106. doi:10.3390/tropicalmed8020106
76. Arora D, Bhatt S, Kumar M, et al. QbD-based rivastigmine tartrate loaded solid lipid nanoparticles for enhanced intranasal delivery to the brain for Alzheimer's therapeutics. *Frontiers in Aging Neuroscience*. 2022;2022:869.
77. Yasir M, Sara UVS, Chauhan I, et al. Solid lipid nanoparticles for nose to brain delivery of donepezil: formulation, optimization by Box–Behnken design, in vitro and in vivo evaluation. *Artif Cells Nanomed Biotechnol*. 2018;46(8):1838–1851.
78. Kataria I, Shende P. Nose-to-brain lipid nanocarriers: an active transportation across BBB in migraine management. *Chemist Phys Lip*. 2022;243:105177. doi:10.1016/j.chemphyslip.2022.105177
79. Yasir M, Chauhan I, Zafar A, et al. Glyceryl behenate-based solid lipid nanoparticles as a carrier of haloperidol for nose to brain delivery: formulation development, in-vitro, and in-vivo evaluation. *Brazil J Pharmaceut Sci*. 2023;2023:58.
80. Yasir M, Chauhan I, Zafar A, et al. Buspirone loaded solid lipid nanoparticles for amplification of nose to brain efficacy: formulation development, optimization by Box-Behnken design, in-vitro characterization and in-vivo biological evaluation. *J Drug Deliv Sci Technol*. 2021;61:102164. doi:10.1016/j.jddst.2020.102164
81. Trapani A, Guerra L, Corbo F, et al. Cyto/biocompatibility of dopamine combined with the antioxidant grape seed-derived polyphenol compounds in solid lipid nanoparticles. *Molecules*. 2021;26(4):916. doi:10.3390/molecules26040916
82. Costa C, Cunha S, Moreira J, et al. Quality by design (QbD) optimization of diazepam-loaded nanostructured lipid carriers (NLC) for nose-to-brain delivery: toxicological effect of surface charge on human neuronal cells. *Internat J Pharmac*. 2021;607:120933. doi:10.1016/j.ijpharm.2021.120933
83. Patel HP, Gandhi PA, Chaudhari PS, et al. Clozapine loaded nanostructured lipid carriers engineered for brain targeting via nose-to-brain delivery: optimization and in vivo pharmacokinetic studies. *J Drug Deliv Sci Technol*. 2021;64:102533. doi:10.1016/j.jddst.2021.102533
84. Masjedi M, Azadi A, Heidari R, Mohammadi-Samani S. Nose-to-brain delivery of sumatriptan-loaded nanostructured lipid carriers: preparation, optimization, characterization and pharmacokinetic evaluation. *J Pharm Pharmacol*. 2020;72(10):1341–1351. doi:10.1111/jphp.13316
85. Nair SC, Vinayan KP, Mangalathillam S. Nose to brain delivery of phenytoin sodium loaded nano lipid carriers: formulation, drug release, permeation and in vivo pharmacokinetic studies. *Pharmaceutics*. 2021;13(10):1640. doi:10.3390/pharmaceutics13101640
86. Torres J, Pereira JM, Marques-Oliveira R, et al. An in vitro evaluation of the potential neuroprotective effects of intranasal lipid nanoparticles containing astaxanthin obtained from different sources: comparative studies. *Pharmaceutics*. 2023;15(4):1035. doi:10.3390/pharmaceutics15041035
87. Sheth T, Seshadri S, Prileszky T, Helgeson ME. Multiple nanoemulsions. *Nat Rev Mater*. 2020;5(3):214–228. doi:10.1038/s41578-019-0161-9

88. Shah B. Microemulsion as a promising carrier for nose to brain delivery: journey since last decade. *J Pharmac Invest*. 2021;2021:1–24.
89. Li M, Du C, Guo N, et al. Composition design and medical application of liposomes. *Europ J Med Chemist*. 2019;164:640–653. doi:10.1016/j.ejmech.2019.01.007
90. Large DE, Abdelmessih RG, Fink EA, Auguste DT. Liposome composition in drug delivery design, synthesis, characterization, and clinical application. *Advan Drug Deliv Rev*. 2021;176:113851. doi:10.1016/j.addr.2021.113851
91. Thapa RK, Kim JO. Nanomedicine-based commercial formulations: current developments and future prospects. *J Pharmaceut Investig*. 2023;53(1):19–33. doi:10.1007/s40005-022-00607-6
92. Ahmed KS, Hussein SA, Ali AH, Korma SA, Lipeng Q, Jinghua C. Liposome: composition, characterisation, preparation, and recent innovation in clinical applications. *J Drug Target*. 2019;27(7):742–761. doi:10.1080/1061186X.2018.1527337
93. Briuglia M-L, Rotella C, McFarlane A, Lamprou DA. Influence of cholesterol on liposome stability and on in vitro drug release. *Drug Deliv Translat Res*. 2015;5(3):231–242. doi:10.1007/s13346-015-0220-8
94. Ryu S, Jin M, Lee H-K, Wang M-H, Baek J-S, Cho C-W. Effects of lipid nanoparticles on physicochemical properties, cellular uptake, and lymphatic uptake of 6-methoxyflavone. *J Pharmaceut Investig*. 2022;52(2):233–241. doi:10.1007/s40005-021-00557-5
95. Geszke-Moritz M, Moritz M. Solid lipid nanoparticles as attractive drug vehicles: composition, properties and therapeutic strategies. *Mater Sci Engin*. 2016;68:982–994. doi:10.1016/j.msec.2016.05.119
96. Salvi VR, Pawar P. Nanostructured lipid carriers (NLC) system: a novel drug targeting carrier. *J Drug Deliv Sci Technol*. 2019;51:255–267. doi:10.1016/j.jddst.2019.02.017
97. Gordillo-Galeano A, Mora-Huertas CE. Solid lipid nanoparticles and nanostructured lipid carriers: a review emphasizing on particle structure and drug release. *Europ J Pharmac Biopharm*. 2018;133:285–308. doi:10.1016/j.ejpb.2018.10.017
98. Abouhussein DM, Khattab A, Bayoumi NA, Mahmoud AF, Sakr TM. Brain targeted rivastigmine mucoadhesive thermosensitive in situ gel: optimization, in vitro evaluation, radiolabeling, in vivo pharmacokinetics and biodistribution. *J Drug Deliv Sci Technol*. 2018;43:129–140. doi:10.1016/j.jddst.2017.09.021
99. Verekar RR, Gurav SS, Bolmal U. Thermosensitive mucoadhesive in situ gel for intranasal delivery of Almotriptan malate: formulation, characterization, and evaluation. *J Drug Deliv Sci Technol*. 2020;58:101778. doi:10.1016/j.jddst.2020.101778
100. Gadhave D, Khot S, Tupe S, et al. Nose-to-brain delivery of octreotide acetate in situ gel for pituitary adenoma: pharmacological and in vitro cytotoxicity studies. *Internat J Pharmac*. 2022;629:122372. doi:10.1016/j.ijpharm.2022.122372
101. Gholizadeh H, Messerotti E, Pozzoli M, et al. Application of a thermosensitive in situ gel of chitosan-based nasal spray loaded with tranexamic acid for localised treatment of nasal wounds. *AAPS Pharm Sci Tech*. 2019;20(7):299. doi:10.1208/s12249-019-1517-6
102. Nair AB, Chaudhary S, Shah H, et al. Intranasal delivery of darunavir-loaded mucoadhesive in situ gel: experimental design, in vitro evaluation, and pharmacokinetic studies. *Gels*. 2022;8(6):342. doi:10.3390/gels8060342
103. Wang Q, Wong C-H, Chan HE, Lee W-Y, Zuo Z. Statistical design of experiment (DoE) based development and optimization of DB213 in situ thermosensitive gel for intranasal delivery. *Internat J Pharmac*. 2018;539(1–2):50–57. doi:10.1016/j.ijpharm.2018.01.032
104. Thakkar H, Vaghela D, Patel BP. Brain targeted intranasal in-situ gelling spray of paroxetine: formulation, characterization and in-vivo evaluation. *J Drug Deliv Sci Technol*. 2021;62:102317. doi:10.1016/j.jddst.2020.102317
105. Nafee N, Ameen AER, Abdallah OY. Patient-friendly, olfactory-targeted, stimuli-responsive hydrogels for cerebral degenerative disorders ensured > 400% brain targeting efficiency in rats. *AAPS Pharm Sci Tech*. 2020;22(1):6. doi:10.1208/s12249-020-01872-0
106. Thakkar JH, Prajapati ST. Formulation development and characterization of in-situ gel of rizatriptan benzoate for intranasal delivery. *J Drug Deliv Ther*. 2021;11(1–s):1–6. doi:10.22270/jddt.v11i1-s.4685
107. Parashar P, Diwaker N, Kanoujia J, et al. In situ gel of lamotrigine for augmented brain delivery: development characterization and pharmacokinetic evaluation. *J Pharm Investig*. 2020;50(1):95–105. doi:10.1007/s40005-019-00436-0
108. Swamy N, Abbas Z. Mucoadhesive in situ gels as nasal drug delivery systems: an overview. *Asian J Pharm Sci*. 2012;7:3.
109. Karavasili C, Fatouros DG. Smart materials: in situ gel-forming systems for nasal delivery. *Drug Discov Today*. 2016;21(1):157–166. doi:10.1016/j.drudis.2015.10.016
110. Watts P, Smith A. PecSys: in situ gelling system for optimised nasal drug delivery. *Expert Opin Drug Deliv*. 2009;6(5):543–552. doi:10.1517/17425240902939135
111. Costa CP, Barreiro S, Moreira JN, et al. In vitro studies on nasal formulations of nanostructured lipid carriers (NLC) and solid lipid nanoparticles (SLN). *Pharmaceuticals*. 2021;14(8):711. doi:10.3390/ph14080711
112. Gao M, Shen X, Mao S. Factors influencing drug deposition in the nasal cavity upon delivery via nasal sprays. *J Pharm Investig*. 2020;50(3):251–259. doi:10.1007/s40005-020-00482-z
113. Nižić L, Ugrina I, Špoljarić D, et al. Innovative sprayable in situ gelling fluticasone suspension: development and optimization of nasal deposition. *Int J Pharm*. 2019;563:445–456. doi:10.1016/j.ijpharm.2019.04.015
114. Castile J, Cheng Y-H, Simmons B, Perelman M, Smith A, Watts P. Development of in vitro models to demonstrate the ability of PecSys®, an in situ nasal gelling technology, to reduce nasal run-off and drip. *Drug Dev Ind Pharm*. 2013;39(5):816–824. doi:10.3109/03639045.2012.707210
115. Perkušić M, Nižić Nodilo L, Ugrina I, et al. Chitosan-based thermogelling system for nose-to-brain donepezil delivery: optimising formulation properties and nasal deposition profile. *Pharmaceutics*. 2023;15(6):1660. doi:10.3390/pharmaceutics15061660
116. Li X, Du L, Chen X, et al. Nasal delivery of analgesic ketorolac tromethamine thermo-and ion-sensitive in situ hydrogels. *Int J Pharm*. 2015;489(1–2):252–260. doi:10.1016/j.ijpharm.2015.05.009
117. Saito S, Ainai A, Suzuki T, et al. The effect of mucoadhesive excipient on the nasal retention time of and the antibody responses induced by an intranasal influenza vaccine. *Vaccine*. 2016;34(9):1201–1207. doi:10.1016/j.vaccine.2016.01.020
118. Watts PJ, Illum L. Inventors; Google Patents, assignee. Pectin compositions and methods of use for improved delivery of drugs to mucosal surfaces. US patent US-6432440-B1; 2002.
119. Chen Y, Cheng G, Hu R, et al. A nasal temperature and pH dual-responsive in situ gel delivery system based on microemulsion of huperzine A: formulation, evaluation, and in vivo pharmacokinetic study. *AAPS PharmSciTech*. 2019;20(7):301. doi:10.1208/s12249-019-1513-x
120. Qu Y, Li A, Ma L, et al. Nose-to-brain delivery of disulfiram nanoemulsion in situ gel formulation for glioblastoma targeting therapy. *Int J Pharm*. 2021;597:120250. doi:10.1016/j.ijpharm.2021.120250

121. Cunha S, Swedrowska M, Bellahnid Y, et al. Thermosensitive in situ hydrogels of rivastigmine-loaded lipid-based nanosystems for nose-to-brain delivery: characterisation, biocompatibility, and drug deposition studies. *Int J Pharm*. 2022;620:121720. doi:10.1016/j.ijpharm.2022.121720
122. Tan MS, Pandey P, Lohman R-J, Falconer JR, Siskind DJ, Parekh HS. Fabrication and characterization of clozapine nanoemulsion sol-gel for intranasal administration. *Mol Pharm*. 2022;19(11):4055–4066. doi:10.1021/acs.molpharmaceut.2c00513
123. Gadhave D, Tupe S, Tagalpallewar A, Gorain B, Choudhury H, Kokare C. Nose-to-brain delivery of amisulpride-loaded lipid-based poloxamer-gellan gum nanoemulgel: in vitro and in vivo pharmacological studies. *Int J Pharm*. 2021;607:121050. doi:10.1016/j.ijpharm.2021.121050
124. Nair AB, Chaudhary S, Jacob S, et al. Intranasal administration of dolutegravir-loaded nanoemulsion-based in situ gel for enhanced bioavailability and direct brain targeting. *Gels*. 2023;9(2):130. doi:10.3390/gels9020130
125. Mura P, Mennini N, Nativi C, Richichi B. In situ mucoadhesive-thermosensitive liposomal gel as a novel vehicle for nasal extended delivery of opiorphin. *Eur J Pharm Biopharm*. 2018;122:54–61. doi:10.1016/j.ejpb.2017.10.008
126. Rajput A, Butani S. Donepezil HCl liposomes: development, characterization, cytotoxicity, and pharmacokinetic study. *AAPS PharmSciTech*. 2022;23(2):74. doi:10.1208/s12249-022-02209-9
127. El-Shenawy AA, Mahmoud RA, Mahmoud EA, Mohamed MS. Intranasal in situ gel of apixaban-loaded nanoethosomes: preparation, optimization, and in vivo evaluation. *AAPS PharmSciTech*. 2021;22(4):147. doi:10.1208/s12249-021-02020-y
128. Ourani-Pourdashti S, Mirzaei E, Heidari R, Ashrafi H, Azadi A. Preparation and evaluation of niosomal chitosan-based in situ gel formulation for direct nose-to-brain methotrexate delivery. *Int J Biol Macromol*. 2022;213:1115–1126. doi:10.1016/j.ijbiomac.2022.06.031
129. Fahmy UA, Badr-Eldin SM, Ahmed OA, et al. Intranasal niosomal in situ gel as a promising approach for enhancing flibanserin bioavailability and brain delivery: in vitro optimization and ex vivo/in vivo evaluation. *Pharmaceutics*. 2020;12(6):485. doi:10.3390/pharmaceutics12060485
130. Abdelnabi DM, Abdallah MH, Elghamry HA. Buspirone hydrochloride loaded in situ nanovesicular gel as an anxiolytic nasal drug delivery system: in vitro and animal studies. *AAPS PharmSciTech*. 2019;20(3):134. doi:10.1208/s12249-018-1211-0
131. Taymouri S, Shahnamnia S, Mesripour A, Varshosaz J. In vitro and in vivo evaluation of an ionic sensitive in situ gel containing nanotransfersomes for aripiprazole nasal delivery. *Pharm Dev Technol*. 2021;26(8):867–879. doi:10.1080/10837450.2021.1948571
132. ElShagea HN, Makar RR, Salama AH, Elkasabgy NA, Basalious EB. Investigating the targeting power to brain tissues of intranasal rasagiline mesylate-loaded transferosomal in situ gel for efficient treatment of Parkinson's disease. *Pharmaceutics*. 2023;15(2):533. doi:10.3390/pharmaceutics15020533
133. Salem HF, Kharshoum RM, Abou-Taleb HA, Naguib DM. Nanosized transferosome-based intranasal in situ gel for brain targeting of resveratrol: formulation, optimization, in vitro evaluation, and in vivo pharmacokinetic study. *AAPS PharmSciTech*. 2019;20(5):181. doi:10.1208/s12249-019-1353-8
134. Uppuluri CT, Ravi PR, Dalvi AV. Design, optimization and pharmacokinetic evaluation of piribedil loaded solid lipid nanoparticles dispersed in nasal in situ gelling system for effective management of Parkinson's disease. *Int J Pharm*. 2021;606:120881. doi:10.1016/j.ijpharm.2021.120881
135. Agrawal M, Pradhan M, Singhvi G, Patel R, Alexander A, Alexander A. Thermoresponsive in situ gel of curcumin loaded solid lipid nanoparticle: design, optimization and in vitro characterization. *J Drug Deliv Sci Technol*. 2022;71:103376. doi:10.1016/j.jddst.2022.103376
136. Abou Youssef NAH, Kassem AA, Farid RM, Ismail FA, Magda Abd Elsamea EM, Boraie NA. A novel nasal almotriptan loaded solid lipid nanoparticles in mucoadhesive in situ gel formulation for brain targeting: preparation, characterization and in vivo evaluation. *Int J Pharm*. 2018;548(1):609–624. doi:10.1016/j.ijpharm.2018.07.014
137. Sun Y, Li L, Xie H, et al. Primary studies on construction and evaluation of ion-sensitive in situ gel loaded with paeonol-solid lipid nanoparticles for intranasal drug delivery. *Int J Nanomed*. 2020;Volume 15:3137–3160. doi:10.2147/IJN.S247935
138. Rajput AP, Butani SB. Resveratrol anchored nanostructured lipid carrier loaded in situ gel via nasal route: formulation, optimization and in vivo characterization. *J Drug Deliv Sci Technol*. 2019;51:214–223. doi:10.1016/j.jddst.2019.01.040
139. Gadhave D, Rasal N, sonawane R, Sekar M, Kokare C. Nose-to-brain delivery of teriflunomide-loaded lipid-based carbopol-gellan gum nanogel for glioma: pharmacological and in vitro cytotoxicity studies. *Int J Biol Macromol*. 2021;167:906–920. doi:10.1016/j.ijbiomac.2020.11.047
140. Taymouri S, Minaiyan M, Ebrahimi F, Tavakoli N. In-vitro and in-vivo evaluation of chitosan-based thermosensitive gel containing lorazepam NLCs for the treatment of status epilepticus. *IET Nanobiotechnol*. 2020;14(2):148–154. doi:10.1049/iet-nbt.2019.0156
141. Tripathi D, Sonar PK, Parashar P, Chaudhary SK, Upadhyay S, Saraf SK. Augmented brain delivery of cinnarizine through nanostructured lipid carriers loaded in situ gel: in vitro and pharmacokinetic evaluation. *BioNanoScience*. 2021;11(1):159–171. doi:10.1007/s12668-020-00821-2
142. Fahmy UA, Ahmed OA, Badr-Eldin SM, et al. Optimized nanostructured lipid carriers integrated into in situ nasal gel for enhancing brain delivery of flibanserin. *Int J Nanomed*. 2020;Volume 15:5253–5264. doi:10.2147/IJN.S258791
143. Rajput A, Bariya A, Allam A, Othman S, Butani SB. In situ nanostructured hydrogel of resveratrol for brain targeting: in vitro-in vivo characterization. *Drug Deliv Transl Res*. 2018;8(5):1460–1470. doi:10.1007/s13346-018-0540-6
144. Abbas H, Refai H, El Sayed N. Superparamagnetic iron oxide-loaded lipid nanocarriers incorporated in thermosensitive in situ gel for magnetic brain targeting of clonazepam. *J Pharm Sci*. 2018;107(8):2119–2127. doi:10.1016/j.xphs.2018.04.007
145. Butani S. Fabrication of an ion-sensitive in situ gel loaded with nanostructured lipid carrier for nose to brain delivery of donepezil. *Asian J Pharm*. 2018;12(04):293–302.
146. Matarazzo AP, Elisei LMS, Carvalho FC, et al. Mucoadhesive nanostructured lipid carriers as a cannabidiol nasal delivery system for the treatment of neuropathic pain. *Eur J Pharm Sci*. 2021;159:105698. doi:10.1016/j.ejps.2020.105698
147. Deshkar SS, Jadhav MS, Shirolkar SV. Development of carbamazepine nanostructured lipid carrier loaded thermosensitive gel for intranasal delivery. *Adv Pharm Bulletin*. 2021;11(1):150–162. doi:10.34172/apb.2021.016
148. Paiva-Santos AC, Silva AL, Guerra C, et al. Ethosomes as nanocarriers for the development of skin delivery formulations. *Pharm Res*. 2021;38(6):947–970. doi:10.1007/s11095-021-03053-5
149. Raghuvanshi A, Shah K, Dewangan HK. Ethosome as antigen delivery carrier: optimisation, evaluation and induction of immunological response via nasal route against hepatitis B. *J Microencapsul*. 2022;39(4):352–363. doi:10.1080/02652048.2022.2084169

150. Natsheh H, Touitou E. Phospholipid vesicles for dermal/transdermal and nasal administration of active molecules: the effect of surfactants and alcohols on the fluidity of their lipid bilayers and penetration enhancement properties. *Molecules*. 2020;25(13):2959. doi:10.3390/molecules25132959
151. Bhardwaj P, Tripathi P, Gupta R, Pandey S. Niosomes: a review on niosomal research in the last decade. *J Drug Deliv Sci Technol*. 2020;56:101581. doi:10.1016/j.jddst.2020.101581
152. Pires PC, Rodrigues M, Alves G, Santos AO. Strategies to improve drug strength in nasal preparations for brain delivery of low aqueous solubility drugs. *Pharmaceutics*. 2022;14(3):588. doi:10.3390/pharmaceutics14030588
153. Sastri KT, Gupta NV, Sharadha M, et al. Nanocarrier facilitated drug delivery to the brain through intranasal route: a promising approach to transcend bio-obstacles and alleviate neurodegenerative conditions. *J Drug Deliv Sci Technol*. 2022;75:103656. doi:10.1016/j.jddst.2022.103656
154. Chamanza R, Wright J. A review of the comparative anatomy, histology, physiology and pathology of the nasal cavity of rats, mice, dogs and non-human primates. Relevance to inhalation toxicology and human health risk assessment. *J Comparat Pathol*. 2015;153(4):287–314. doi:10.1016/j.jcpa.2015.08.009
155. Zahir-Jouzdani F, Wolf JD, Atyabi F, Bernkop-Schnürch A. In situ gelling and mucoadhesive polymers: why do they need each other? *Expert Opinion on Drug Deliv*. 2018;15(10):1007–1019. doi:10.1080/17425247.2018.1517741
156. Yadav S, Gattacceca F, Panicucci R, Amiji MM. Comparative biodistribution and pharmacokinetic analysis of cyclosporine-A in the brain upon intranasal or intravenous administration in an oil-in-water nanoemulsion formulation. *Molec Pharmaceut*. 2015;12(5):1523–1533. doi:10.1021/mp5008376
157. Lim C, Koo J, Oh KT. Nanomedicine approaches for medulloblastoma therapy. *J Pharmac Investig*. 2023;53(2):213–233. doi:10.1007/s40005-022-00597-5
158. Lee S-H, Kim J-K, Jee J-P, Jang D-J, Park Y-J, Kim J-E. Quality by Design (QbD) application for the pharmaceutical development process. *J Pharmac Investig*. 2022;52(6):649–682. doi:10.1007/s40005-022-00575-x
159. Cunha S, Costa CP, Moreira JN, Lobo JMS, Silva AC. Using the quality by design (QbD) approach to optimize formulations of lipid nanoparticles and nanoemulsions: a review. *Nanomedicine*. 2020;28:102206. doi:10.1016/j.nano.2020.102206
160. Rathore AS. Roadmap for implementation of quality by design (QbD) for biotechnology products. *Trend Biotechnol*. 2009;27(9):546–553. doi:10.1016/j.tibtech.2009.06.006
161. Soni G, Kale K, Shetty S, Gupta M, Yadav KS. Quality by design (QbD) approach in processing polymeric nanoparticles loading anticancer drugs by high pressure homogenizer. *Heliyon*. 2020;6(4):e03846. doi:10.1016/j.heliyon.2020.e03846
162. Li J, Qiao Y, Wu Z. Nanosystem trends in drug delivery using quality-by-design concept. *J Controll Rel*. 2017;256:9–18. doi:10.1016/j.jconrel.2017.04.019